Geochronological constraints on granitic magmatism, deformation, cooling and uplift on Bornholm, Denmark

TOD E. WAIGHT, DIRK FREI & MICHAEL STOREY

Waight, T.E., Frei, D. & Storey, M. 2012. Geochronological constraints on granitic magmatism, deformation, cooling and uplift on Bornholm, Denmark. © 2012 by Bulletin of the Geological Society of Denmark, Vol. 60, pp. 23–46. ISSN 0011–6297 (www.2dgf.dk/publikationer/bulletin). https://doi.org/10.37570/bgsd-2012-60-03

U-Pb ages on zircon from 11 samples of granitoid and gneiss from the Danish island of Bornholm have been obtained using laser ablation - inductively coupled plasma mass spectrometry. These ages indicate that the felsic basement rocks were generated over a restricted period in the Mesoproterozoic at 1455 ± 10 Ma. No evidence has been found for the presence of 1.8 Ga basement gneisses as observed to the north in southern Sweden and as inferred in previous studies. No distinction in age can be made between relatively undeformed granitic lithologies and gneissic lithologies within the errors of the technique. This indicates that granitic magmatism, deformation and metamorphism all occurred within a relatively restricted and contemporaneous period. The granitic magmatism on Bornholm can thus be correlated to similar events at the same time in southern Sweden, Lithuania, and elsewhere in Baltica, and is therefore part of a larger magmatic event affecting the region. Argon and Rb-Sr ages on various minerals from a single sample of the Rønne Granite provide constraints on the cooling and uplift history of the basement in the region. Using recently published closure temperatures for each isotopic system a cooling curve is generated that illustrates a period of rapid cooling immediately after and/or during crystallisation. This likely represents the period of emplace-ment, crystallisation, and deformation of the felsic basement. The modelled rate of post-emplacement cooling is highly dependent on the choice of closure temperature for Ar isotopes in biotite. Use of recently published values of around 450°C defines a prolonged period of slower cooling (*c.* 4°C per million years) over nearly 100 million years down to *c.* 300°C and the closure temperature of Sr iso-topes in biotite. Use of older and lower closure temperatures defines curves that are more consistent with theoretical models. The low closure temperature of Sr isotopes in biotite explains much of the wide variation in previous age determinations using various techniques on Bornholm. There is no evidence in the geochronological data for disturbance during later tectonic events in the region.

Keywords: Bornholm, geochronology, zircon, granitoid, gneiss, Danolopolian, Rb-Sr, ^{40}Ar-^{39}Ar.

Tod Waight [todw@geo.ku.dk], Department of Geography and Geology, University of Copenhagen, Øster Voldgade 10, DK-1350 Copenhagen K, Denmark. Dirk Frei, Geological Survey of Denmark and Greenland (GEUS), Øster Voldgade 10, DK-1350 Copenhagen K, Denmark; presently at Department of Earth Sciences, Corner Ryneveld and Merriman Streets, Stellenbosch, Private Bag X1, Matieland, 7602, South Africa. Michael Storey, QUADLAB, Department of Environmental, Social and Spatial Change, Roskilde University, Universitetsvej 1, DK-4000 Roskilde, Denmark.

Received 10 January 2012
Accepted in revised form
9 May 2012
Published online
15 June 2012

The only exposures of basement rocks in Denmark are found on Bornholm and comprise high-grade gneisses and intrusive granitoids (Callisen 1934; Micheelsen 1961; Berthelsen 1989). Bornholm is strategically important within the plate tectonic framework of Northern Europe, representing a link between the basement exposures of southern Sweden and the buried basement of northeast Poland and Lithuania. Structurally, Bornholm lies within the Tornquist zone, a complex large scale shear zone running between Sweden and Denmark and separating the old, thick cold crust of north-eastern Europe (Fennoscandia) from the hotter, thinner crust of the younger mobile belts of central and western Europe (e.g. Gorbatschev & Bogdanova 1993; Graversen 2009). Therefore, a better understanding of the geological evolution of this region is vital to a large-scale understanding of northern Europe.

Early studies proposed that all felsic basement lithologies on Bornholm (granites and gneisses) were chemically related, and therefore by inference

also contemporaneous (Callisen 1934). Micheelsen (1961) described a geological history beginning with a geosynclinal sequence of sediments and basalts that was progressively and variably granitised under granulitic then amphibolitic facies conditions (Rønne and Hammer stages respectively), simultaneous with the generation of foliations and both large and smaller scale folding. Post-kinematic granitisation resulted in formation of the Svaneke Granite although no specific time constraints were suggested for how the various granitisation episodes were related to each other. To the north of Bornholm, in the Blekinge Province of SE Sweden, geological and geochronological investigations identified a series of older (*c.* 1.8–1.7 Ga) basement gneiss lithologies (Tving granitoid and Västanå Formation) intruded by younger granitoids dated at around 1.45 Ga (Åberg 1988; Johansson & Larsen 1989; Kornfält 1993, 1996). Early K-Ar age determinations on Bornholm granites ranged between 1.4 and 1.25 Ga (Larsen 1971) and suggested a link between the granites on Bornholm and in SE Sweden. Based on these ages, and previous work, Berthelsen (1989) suggested two loosely constrained episodes of granitoid magmatism on Bornholm, an older phase at *c.* 1780–1650 Ma (e.g. gneiss and Rønne Granite) and a younger phase at *c.* 1400 Ma. More recent studies suggest that all the granitoids were emplaced over a relatively short time span (1470–1440 Ma) (Obst *et al.* 2004 and references therein; Zariņš & Johansson 2009), and no age distinction can be made between undeformed granitoids, deformed granitoids, and gneisses. These age ranges strongly suggest that the Bornholm granitoids can be correlated with rocks from the Blekinge Province in southern Sweden (Obst *et al.* 2004) and are part of a much larger province of intracratonic magmatism (e.g. Bogdanova *et al.* 2008).

In this study, we present new laser ablation - inductively coupled plasma mass spectrometry (LA-ICPMS) U-Pb zircon ages for 11 granitoids and gneisses from Bornholm. Several of these samples come from the same or similar localities dated using secondary ion mass spectrometry (SIMS) by Zariņš & Johansson (2009) and this provides an excellent opportunity to confirm these earlier results and to compare the two techniques. These authors also identified a number of older (inherited) zircons in several of their samples. In

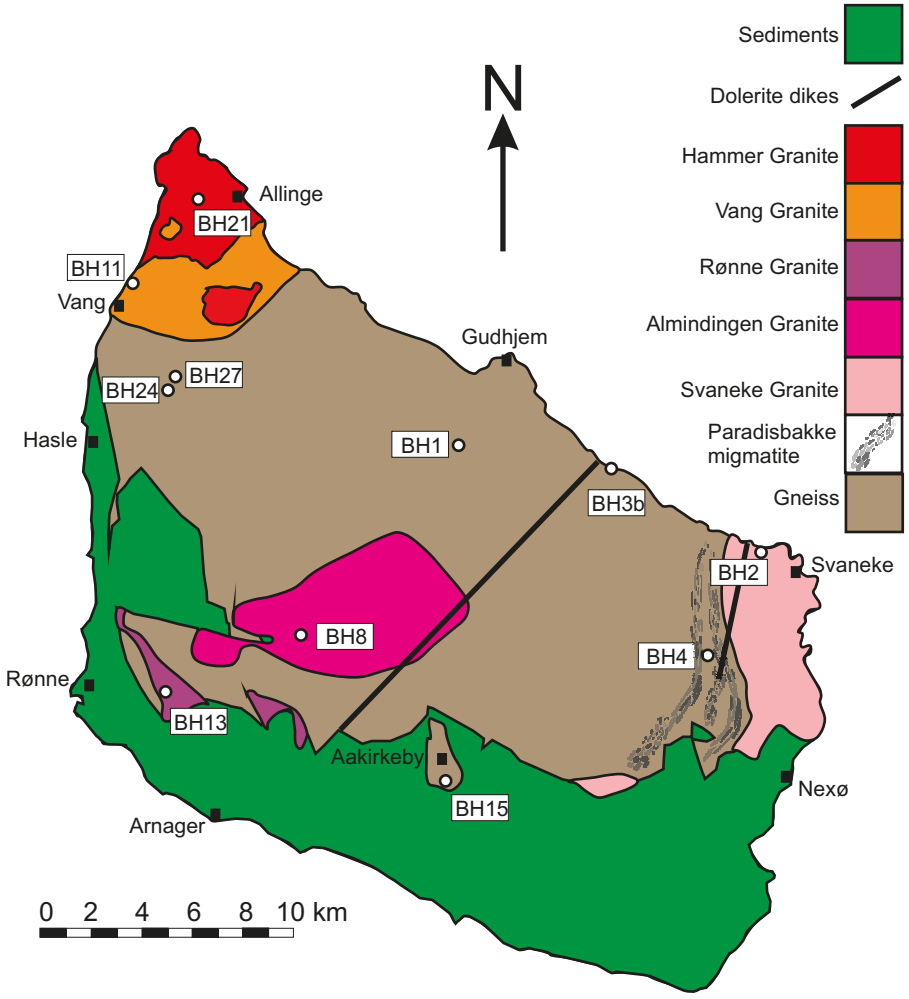

Fig 1: Location map, with sample localities and summary basement geology of Bornholm (modified from Berthelsen 1989). The Maegård Granite (sample BH24) is a small isolated outcrop and is not shown at the scale of this map.

light of this, we also analysed a larger population of zircons in several of the gneissic samples to more closely examine the inherited zircon population on Bornholm and provide constraints on potential source rocks and deeper crustal lithologies under Bornholm. Finally, we present a detailed geochronological study of a single sample, utilising a number of isotopic systems with distinct closure temperatures to attempt to establish a cooling path for the Bornholm basement.

Geological overview

The general geology of the granitoids of Bornholm was described in detail by Callisen (1934) and Micheelsen (1961); more recent detailed descriptions of the petrography and field relationships of the Bornholm granitoids and gneisses are summarised by Berthelsen (1989), Gravesen (1996), Obst *et al.* (2004), and Zariņš & Johansson (2009). Previous geochronological investigations on Bornholm have been succinctly summarised by Obst *et al.* (2004) and Zariņš & Johansson (2009). Berthelsen (1989) suggested that the gneissic basement on Bornholm was equivalent to the subduction-related 1.8 Ga gneisses exposed to the north in Sweden. These were then intruded by a series of older granitoids, and the entire sequence was subsequently deformed and folded. A series of younger granitoids were then emplaced and later deformed. In detail, at least six separate granitoid intrusions have been identified: Almindingen Granite, Hammer Granite, Maegård Granite, Rønne Granite, Svaneke Granite and Vang Granite (Fig. 1). The basement rocks on Bornholm are also intruded by a series of mafic dikes, which have recently been discussed in detail by Holm *et al.* (2010). Four distinct episodes of dike emplacement (1326 Ma, 1220 Ma, 950 Ma, and 300 Ma) are identified.

Zariņš & Johansson (2009) found no evidence for an older 1.8 Ga basement component on Bornholm, or two distinct granitic events. All units (both granitoid and gneiss) were found to have been emplaced in the Mesoproterozoic between 1.47 and 1.44 Ga. Of the gneissic basement that was previously considered to be 1.8 Ga, only two gneiss samples, together with the Paradisbakke Migmatite, yielded reliable U-Pb ages in the Zariņš & Johansson (2009) study. We therefore present ages for several new gneissic samples from different locations than those investigated by Zariņš & Johansson (2009). The small yet distinct Maegård intrusion has not been previously dated and therefore we also present an age for this unit. Table 1 gives details of the location and petrography of the samples investigated in this study.

Methods

Sample preparation and imaging

Samples were crushed and sieved and zircons were separated using conventional heavy liquid methods. The zircons were then handpicked and mounted in 1-inch round epoxy mounts, ground to approximately 60–75% of their thickness and polished to 1-micron grade. Prior to analysis the zircons were imaged in order to identify potential zoning, inherited cores, metamictization and other internal structures using backscattered electron (BSE) imaging on the JEOL JXA-8200 Superprobe at the Department of Geography and Geology, University of Copenhagen.

U-Pb geochronology

U-Pb dating was carried out by LA-ICPMS at GEUS in Copenhagen, using a double focusing Thermo-Finnigan Element2 SF mass spectrometer coupled to a NewWave UP213 frequency quintupled laser ablation system and analytical techniques described in detail by Gerdes & Zeh (2006) and Frei & Gerdes (2009). All analyses were obtained by single spot analysis with a spot diameter of 30 μm and a crater depth of approximately 15–20 μm. All analyses were pre-programmed and laser-induced elemental fractional and instrumental mass discrimination were corrected based on regular analyses of the reference zircon (GJ-1; Simon *et al.* 2004); two GJ-1 analyses were made for every ten sample zircon spots. For quality control the Plešovice zircon standard (Nasdala *et al.* 2008) was analysed regularly and yielded a concordia age of 338.8 ± 1.1 Ma (n = 28; MSWD of concordance and equivalence = 0.44), in good agreement with the published ID-TIMS $^{206}Pb/^{238}U$ age of 337.1 ± 0.4 Ma (Sláma *et al.* 2008). Calculation of concordia ages and plotting of concordia diagrams were carried out using Isoplot/Ex. 3.0 (Ludwig 2003). Unless stated otherwise, all ages are calculated using only those analyses that have the highest degree of concordance, i.e. are within the range of 97–103% concordant. A larger number of zircon analyses (*c.* 100) were made for several gneiss samples in order to asses the possibility of inheritance and the age of inherited populations. These data are presented as age probability diagrams constructed using AgeDisplay (Sircombe 2004).

Rb-Sr geochronology

Sr isotopic compositions and Rb and Sr concentrations were determined on biotite, feldspar (predominantly Na-rich plagioclase), and amphibole separates, and a whole rock powder from sample BH13 (Rønne

Granite). Mineral separates were produced using conventional heavy liquid and magnetic separations. The separates were hand-picked to remove impurities and then cleaned in MQ-water, weighed into Teflon beakers, and an appropriate amount of mixed ^{87}Rb-^{84}Sr tracer was added to each sample. Mineral and whole rock samples were then dissolved using standard HF-HCl-HNO_3 procedures and Rb and Sr were separated using techniques described by Waight *et al.* (2002a). Sr aliquots were loaded on single Ta filaments and analysed in multi-dynamic mode on the VG Sector 54 thermal ionisation mass spectrometer (TIMS) at the Department of Geography and Geology, University of Copenhagen. Rb was loaded in a similar fashion and run on the same instrument in static mode. Analysis of the SRM987 standard during the analytical session gave 0.71024 ± 1 (n=2) which is in perfect agreement with the long-term reproducibility in the laboratory.

^{40}Ar-^{39}Ar geochronology

^{40}Ar-^{39}Ar ages were determined at the Quaternary Dating Laboratory, Roskilde University, Denmark, on splits of the same biotite and amphibole separates analysed for Sr isotope composition. Samples were irradiated for 40 h in the CLICIT facility of the Oregon State University TRIGA reactor along with Fish Canyon sanidine (FCs-2; 28.172 Ma; Rivera *et al.*, 2011) as the neutron-fluence monitor mineral. The argon isotopic analyses were made on a fully automated Nu Instruments Noblesse multi-collector noble-gas mass spectrometer following protocols and corrections for interference isotopes detailed in Brumm *et al.* (2010) and Rivera *et al.* (2011). Step heating experiments were carried out using a 50-W Synrad CO_2 laser in conjunction with an integrator lens that delivered a *c.* 5 mm^2 square beam, with top hat energy profile, to the sample. The quoted uncertainties on the ^{40}Ar-^{39}Ar ages are experimental errors including the error on J (the neutron flux parameter), but do not include potential uncertainties on the ^{40}K decay constant.

Results

Zircon ages

Eleven samples were dated in this study; their locations and brief petrographic descriptions of the dated samples are given in Table 1. Analyses of representative concordant zircons are presented in Table 2 and the full data set is available as an electronic appendix at the web site http://2dgf.dk/publikationer/bulletin/192bull60.html or can be requested from the first author. Back-scattered electron images of representative zircons from each sample, together with concordia diagrams, are presented in Fig. 2 A–K.

BH1: Amphibole gneiss, Knarregård
This sample is typical of the grey, amphibole-bearing granitic orthogneisses that make up much of the basement exposures on Bornholm. In thin section the rock comprises anhedral to subhedral quartz up to *c.* 0.5

Table 1. Details of sample locations and brief sample descriptions

Sample	Unit[1]	Location	Description
BH1	Gneiss	Knarregård Quarry, 55°10′55.8″N, 14°56′17.8″E	Grey, medium-grained, foliated, equicrystalline hornblende-biotite orthogneiss
BH3b	Gneiss	Saltuna, 55°10′34.3″N, 15°1′21.3″E	Red, medium-grained, foliated, equicrystalline biotite gneiss
BH4	Paridisbakke migmatite	Præstebo Quarry, 55°6′13.1″N, 15°5′24.1″E	Grey, mesocratic, medium to coarse-grained, foliated hornblende-biotite gneiss/ migmatite with leucocratic veins
BH6	Svaneke Granite	Listed, Gulehald 55°8′42.2″N, 15°6′51.8″E	Red, coarse-grained, equicrystalline biotite granite
BH8	Almindingen Granite	Bjergebakke Quarry 55°7′8.1″N, 14°49′49.1″E	Red, leucocratic, medium-grained biotite granite
BH11	Vang Granite	Vang quarry 55°14′42.2″N, 14°44′5.5″E	Grey, mesocratic, medium-grained, equicrystalline biotite granite
BH13	Rønne Granite	Stubbegård quarry 55°6′11.4″N, 14°44′37.2″E	Grey, mesocratic, medium to coarse-grained equicrystalline biotite-hornblende granite
BH15	Gneiss	NaturBornholm 55°3′55.8″N, 14°55′2.0″E	White-pink, coarse-grained, equicrystalline biotite granite cut by numerous pegmatites displaying graphic intergrowths
BH21	Hammer Granite	Moseløkken quarry 55°16′24.4″N, 14°46′29.2″E	White-pink, leucocratic, medium-grained, equicrystalline biotite granite
BH24	Maegård Granite	Maegård 55°12′23.0″N, 14°45′17.0″E	Grey, mesocratic, fine-grained, porphyritic hornblende granite
BH27	Gneiss	Rutsker 55°12′41.2″N, 14°45′34.8″E	Red, leucocratic, medium-grained, equicrystalline, foliated biotite gneiss

1: unit names follow the terminology proposed by Berthelsen (1989).

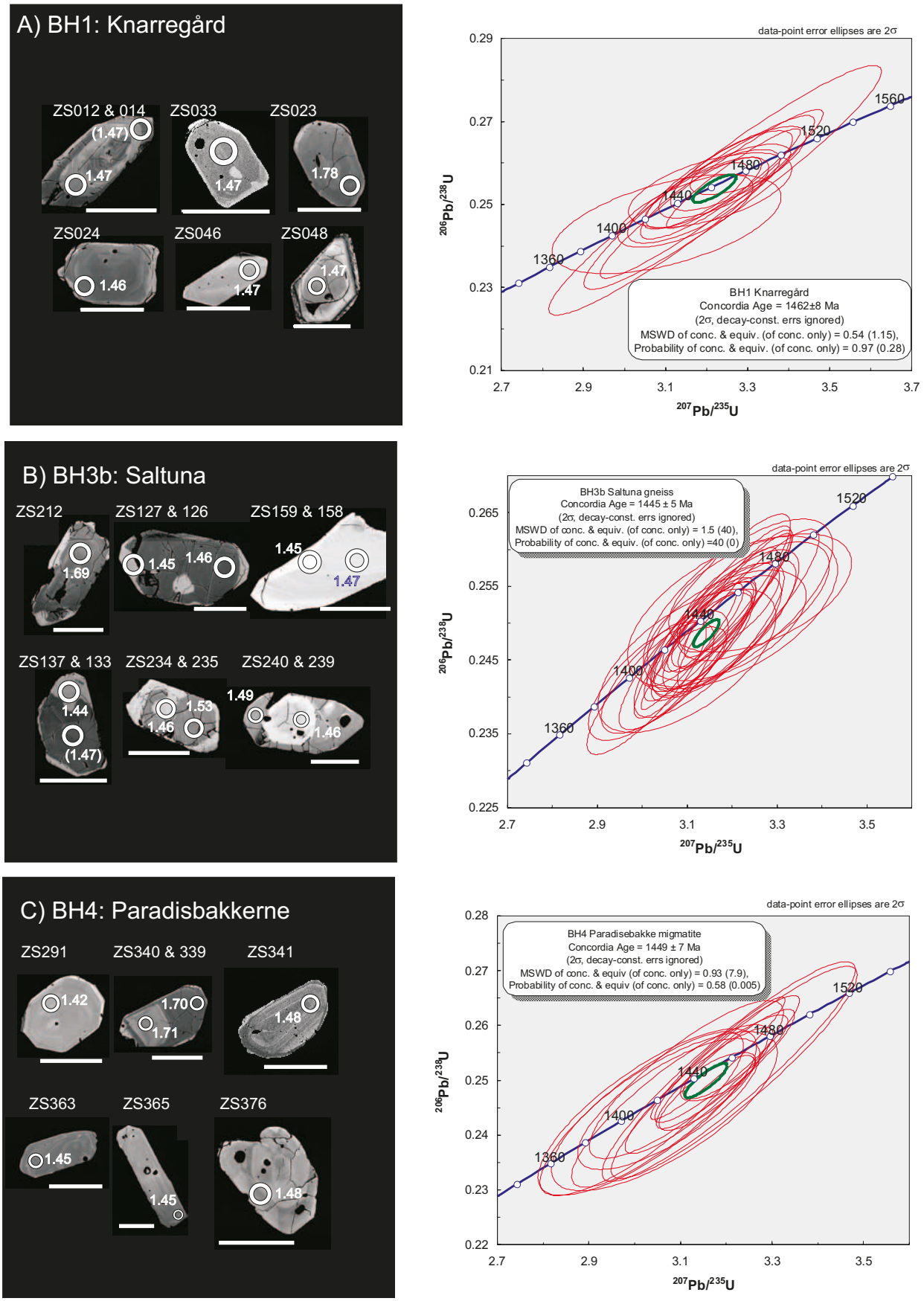
A) BH1: Knarregård
ZS012 & 014
ZS033
ZS023
ZS024
ZS046
ZS048
B) BH3b: Saltuna
ZS212
ZS127 & 126
ZS159 & 158
ZS137 & 133
ZS234 & 235
ZS240 & 239
C) BH4: Paradisbakkerne
ZS291
ZS340 & 339
ZS341
ZS363
ZS365
ZS376
data-point error ellipses are 2σ
BH1 Knarregård
Concordia Age = 1462±8 Ma
(2σ, decay-const. errs ignored)
MSWD of conc. & equiv. (of conc. only) = 0.54 (1.15),
Probability of conc. & equiv. (of conc. only) = 0.97 (0.28)
BH3b Saltuna gneiss
Concordia Age = 1445 ± 5 Ma
(2σ, decay-const. errs ignored)
MSWD of conc. & equiv. (of conc. only) = 1.5 (40),
Probability of conc. & equiv. (of conc. only) =40 (0)
BH4 Paradisebakke migmatite
Concordia Age = 1449 ± 7 Ma
(2σ, decay-const. errs ignored)
MSWD of conc. & equiv (of conc. only) = 0.93 (7.9),
Probability of conc. & equiv (of conc. only) = 0.58 (0.005)
206Pb/238U
207Pb/235U

Fig. 2 A-C.

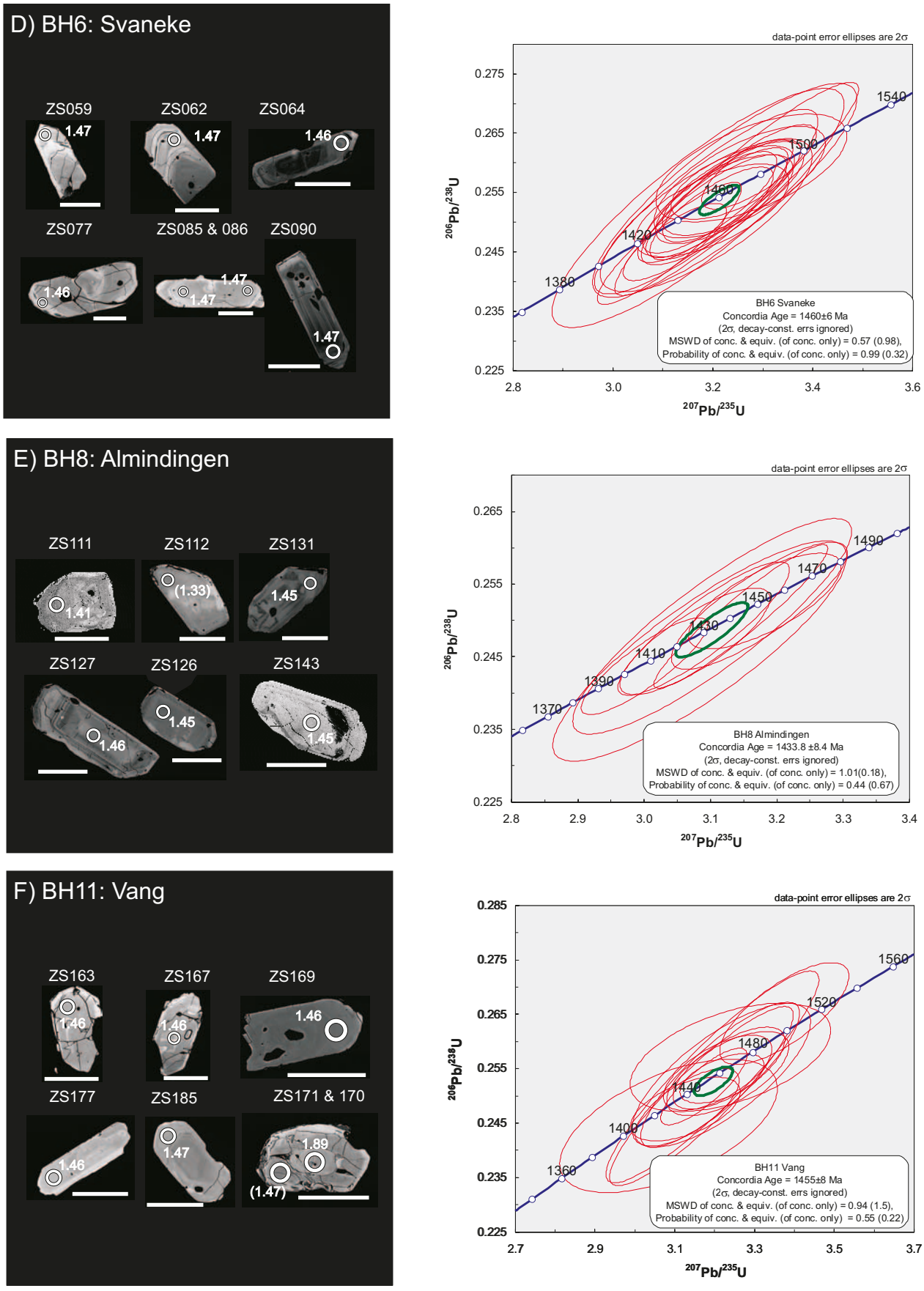
D) BH6: Svaneke
ZS059
ZS062
ZS064
ZS077
ZS085 & 086
ZS090
1.47
1.47
1.46
1.46
1.47
1.47
1.47
data-point error ellipses are 2σ
BH6 Svaneke
Concordia Age = 1460±6 Ma
(2σ, decay-const. errs ignored)
MSWD of conc. & equiv. (of conc. only) = 0.57 (0.98),
Probability of conc. & equiv. (of conc. only) = 0.99 (0.32)
E) BH8: Almindingen
ZS111
ZS112
ZS131
ZS127
ZS126
ZS143
1.41
(1.33)
1.45
1.46
1.45
1.45
data-point error ellipses are 2σ
BH8 Almindingen
Concordia Age = 1433.8 ±8.4 Ma
(2σ, decay-const. errs ignored)
MSWD of conc. & equiv. (of conc. only) = 1.01(0.18),
Probability of conc. & equiv. (of conc. only) = 0.44 (0.67)
F) BH11: Vang
ZS163
ZS167
ZS169
ZS177
ZS185
ZS171 & 170
1.46
1.46
1.46
1.46
1.47
1.89
(1.47)
data-point error ellipses are 2σ
BH11 Vang
Concordia Age = 1455±8 Ma
(2σ, decay-const. errs ignored)
MSWD of conc. & equiv. (of conc. only) = 0.94 (1.5),
Probability of conc. & equiv. (of conc. only) = 0.55 (0.22)

Fig. 2 D-F.

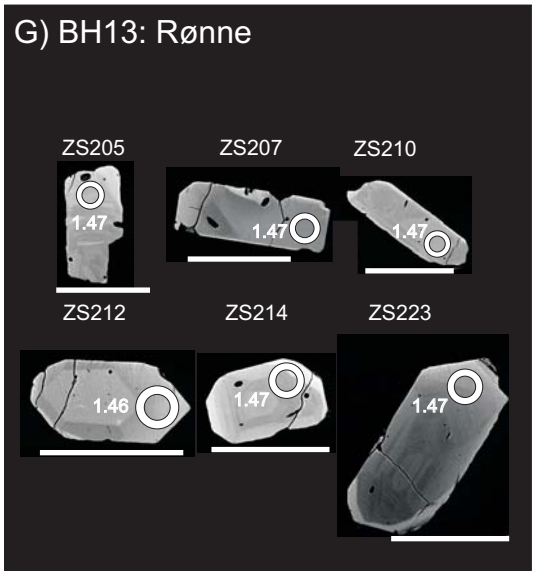
G) BH13: Rønne
ZS205
ZS207
ZS210
1.47
1.47
1.47
ZS212
ZS214
ZS223
1.46
1.47
1.47

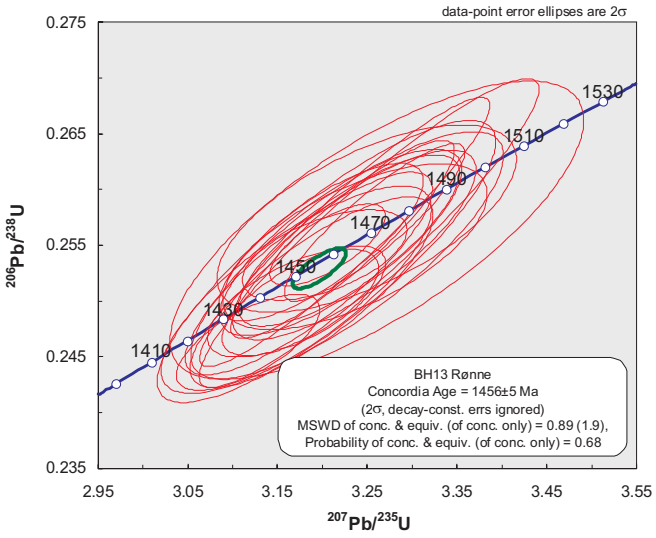
data-point error ellipses are 2σ
BH13 Rønne
Concordia Age = 1456±5 Ma
(2σ, decay-const. errs ignored)
MSWD of conc. & equiv. (of conc. only) = 0.89 (1.9),
Probability of conc. & equiv. (of conc. only) = 0.68
206Pb/238U
207Pb/235U

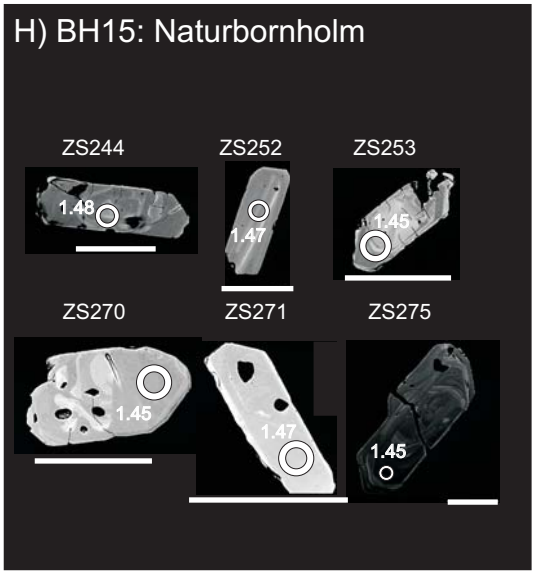
H) BH15: Naturbornholm
ZS244
ZS252
ZS253
1.48
1.47
1.45
ZS270
ZS271
ZS275
1.45
1.47
1.45

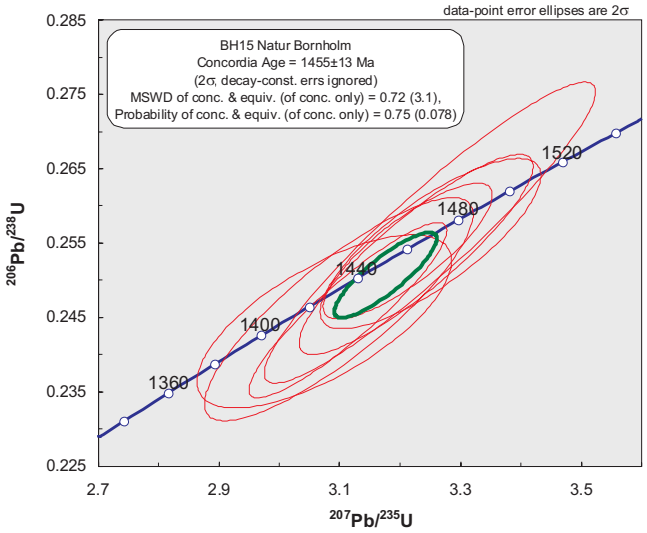
data-point error ellipses are 2σ
BH15 Natur Bornholm
Concordia Age = 1455±13 Ma
(2σ, decay-const. errs ignored)
MSWD of conc. & equiv. (of conc. only) = 0.72 (3.1),
Probability of conc. & equiv. (of conc. only) = 0.75 (0.078)
206Pb/238U
207Pb/235U

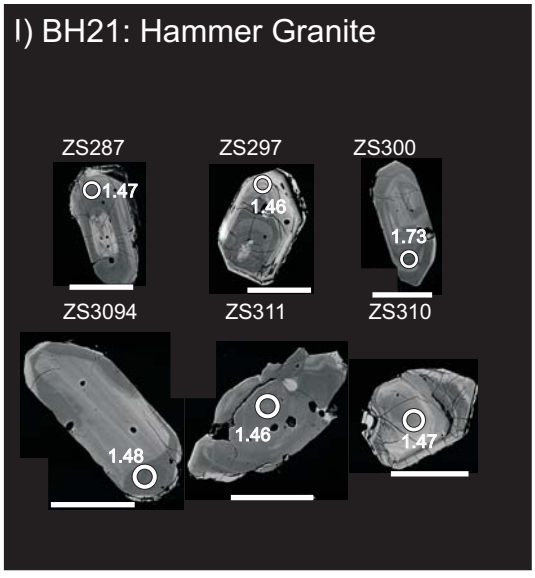
I) BH21: Hammer Granite
ZS287
ZS297
ZS300
1.47
1.46
1.73
ZS3094
ZS311
ZS310
1.48
1.46
1.47

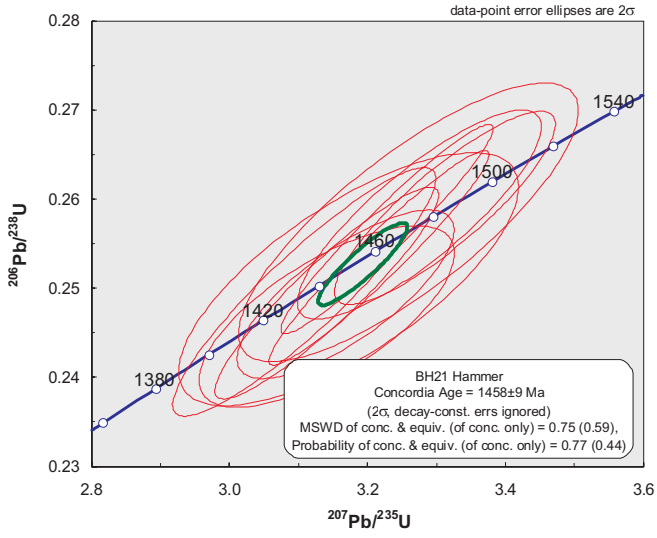
data-point error ellipses are 2σ
BH21 Hammer
Concordia Age = 1458±9 Ma
(2σ, decay-const. errs ignored)
MSWD of conc. & equiv. (of conc. only) = 0.75 (0.59),
Probability of conc. & equiv. (of conc. only) = 0.77 (0.44)
206Pb/238U
207Pb/235U

Fig. 2 G-I.

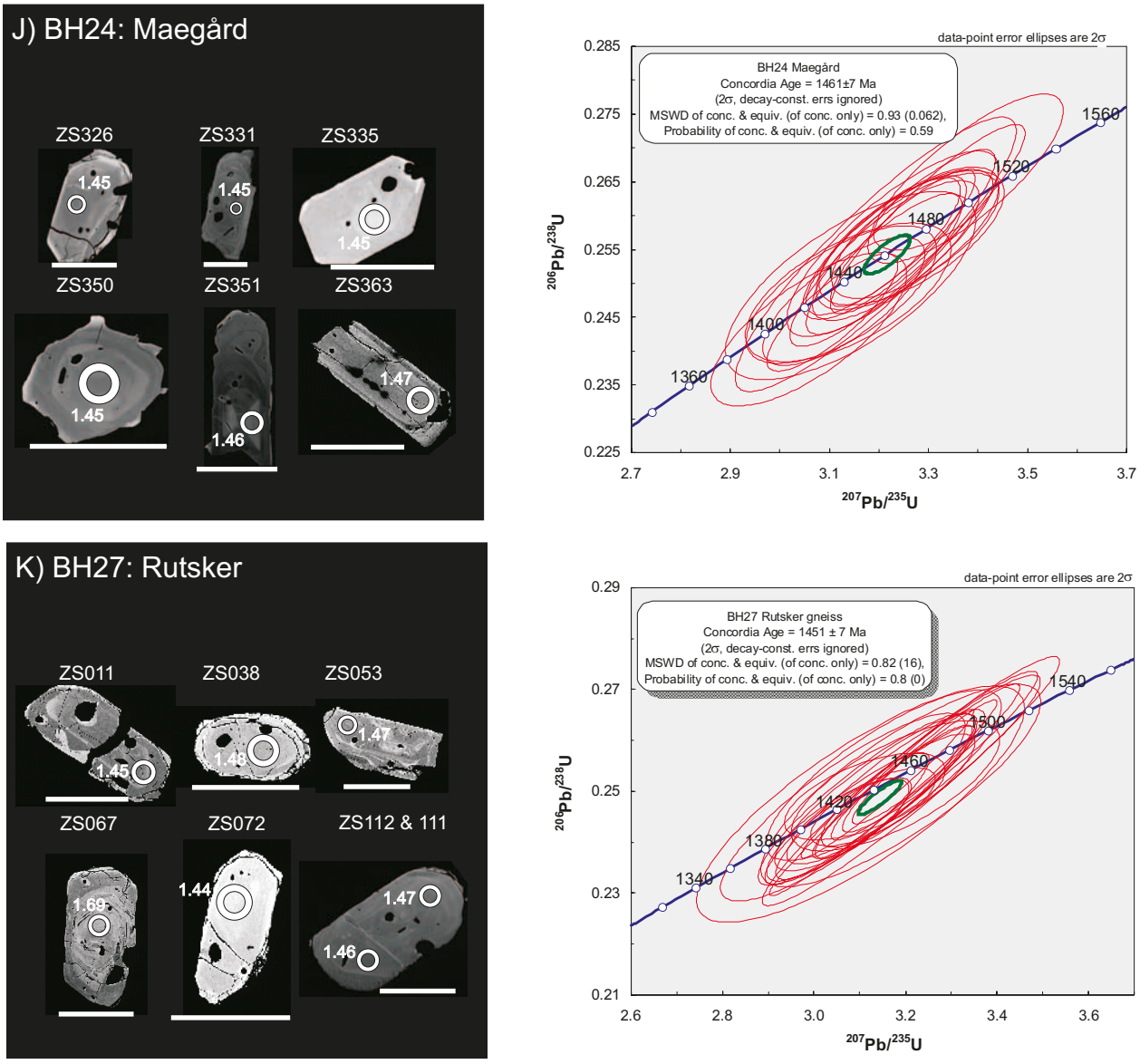

◀▲ Fig 2: Selected BSE images of representative zircons, and concordia ages for all samples investigated in this study. Numbers prefixed 'ZS' above individual zircon images correspond to analyses in Table 2 and the electronic appendix (e.g. for sample BH1, analysis ZS012 refers to Spot-Name 'zircon_sample-012'). Ages on BSE images are $^{207}Pb/^{206}Pb$ ages (in Ga) for individual spot analyses and typically have errors on the order of 0.03–0.05 Ga. Most ages shown are within the range of 97–103% concordant; slightly discordant ages (none less than 93% concordant) are given in brackets. Representative inherited grains are also shown if appropriate. Scale on all zircons = 100 μm, circle represents a spot size of 30 μm. Concordia plots were generated in Isoplot (Ludwig 2003): all ages are calculated using only analyses that are 97-103% concordant, and excluding potentially inherited grains. The small green ellipses represent the calculated age and weighted mean error ellipses.

mm in diameter exhibiting minor undulous extinction, abundant anhedral alkali feldspar crystals up to 0.5 mm across with near-ubiquitous cross-hatch twinning, and plagioclase as generally larger (up to *c.* 2mm) anhedral to subhedral albite-twinned crystals commonly displaying minor sericitisation. Mafic minerals generally occur in clusters and are aligned, defining a relatively strong foliation. They consist of light brown to green pleochroic biotite, occurring as anhedral crystals up to 0.5 mm long, and anhedral light brown to green-to-green-blue pleochroic amphibole crystals up to 0.5 mm in length. Also present are anhedral crystals of titanite up to 0.5 mm in diameter, commonly associated with and surrounding relatively abundant subhedral opaque phases up to 0.5 mm in diameter. Accessory minerals include relatively large (up to 0.5 mm) and abundant apatite and zircon.

Zircons from this sample are typically stubby euhedral crystals 100–200 μm in size and with width to length ratios of *c.* 1:2. Many of the zircons are relatively unzoned particularly in their cores, whereas others show relatively complex growth zoning. Occasional examples with rounded, potentially inherited cores are observed. Representative images are presented in Fig. 2A.

Thirty-two zircons were dated from this sample. Six of these were identified as inherited and have $^{207}Pb/^{206}Pb$ ages that scatter between 1.5 Ga (n=2), 1.6 Ga (n=2) and 1.7 Ga (n=2). The inherited zircons exist either as independent, relatively unzoned anhedral to rounded crystals, or as unzoned cores with thin zoned rims. A number of zircons also show evidence for Pb loss and are discordant; these are typically analyses from the rims of grains. The remaining zircons that are 97–103% concordant define an age of 1462 ± 8 Ma (Fig. 2A); this age is identical to a SIMS age determined on a sample from the same location by Zariņš & Johansson (2009).

BH3b: Gneiss, Saltuna

This sample is a granitic orthogneiss collected on the northern coast *c.* 50 m east of the large doleritic dike at Kelseå. Petrographically, the sample consists of anhedral to subhedral quartz crystals up to 0.25 mm in diameter and displaying weak undulous extinction, patchily zoned and sericitised crystals of anhedral to subhedral plagioclase up to 4 mm in length and containing abundant biotite inclusions, and anhedral crystals of alkali feldspar up to 0.5 mm across characterized by abundant cross hatch twinning. Mafic phases occur in oriented bands and define the foliation in the rock. They comprise yellow to brown pleochroic anhedral crystals of biotite up to *c.* 0.25 mm in length and light green to dark green pleochroic anhedral crystals of amphibole up to 0.25 mm long. Titanite is present as relatively small (*c.* 0.1 mm) anhedral crystals, typically occurring in clusters with, or rimming, anhedral opaque phases. Zircon and apatite occur as accessory phases.

Zircons in this sample are typically stubby, subhedral to euhedral crystals around 100–200 μm in size and with width to length ratios of 1:2. Relatively dark, homogeneous or magmatically zoned cores are common and often display evidence for resorption. Thinner brighter rims with some complex magmatic zoning typically surround these. Some rounded, possibly inherited, cores are also evident. The thin bright rims were generally too small to analyse with a 30 μm spot, although a few partial analyses were possible; these did not yield distinctly different ages from cores. Representative images are presented in Fig. 2B.

About 100 zircons were analysed from this sample, *c.* half of these are more than 3% discordant and are excluded from the final age calculation; they suggest small amounts of Pb loss. Of the entire zircon population analysed, only 11 were considered to be possibly inherited; these have $^{207}Pb/^{206}Pb$ ages clustering at 1.5 (n=8), 1.6 (n=2) and 1.7 Ga (n=1). The remaining zircons (n=30) define a slightly discordant age of 1445 ± 5 Ma (MSWD = 1.5) (Fig. 2B).

BH4: Paradisbakke Migmatite

The Paradisbakke Migmatite displays field evidence for partial melting; however, no physical separation of leucosome from mesosome was attempted in this study. In thin section, the analysed sample is broadly syenogranitic, exhibits only a weak foliation, and includes anhedral crystals of quartz up to 2 mm across and displaying undulous extinction, anhedral to subhedral crystals of plagioclase up to 2mm in length and displaying albite twins and some sericitisation. Abundant alkali feldspar occurs as anhedral, cross-hatch twinned grains typically up to *c.* 1 mm in length, although occasional larger (up to 4 mm) perthitic crystals also occur. Mafic minerals comprise subequal proportions of yellow to brown pleochroic biotite, present as anhedral crystals up to 0.5 mm in diameter, and anhedral light-green to green to blue-green pleochroic crystals of amphibole up to 0.5 mm in length. Opaque phases and titanite are relatively rare and zircon and apatite occur as accessory phases.

The zircons in this sample are typically euhedral to sub-rounded stubby crystals 100–200 μm long, with width to length ratios of 1:2, although longer crystals that are more prismatic are also present. Many show homogeneous or magmatically zoned cores, surrounded by thin rims. There is little evidence in the morphology for partial melting and distinct zircon populations from leucosome and mesosome. The few inherited zircons identified do not show any distinctive morphological features enabling simple discrimination from magmatic zircons. Representative BSE images are presented in Fig. 2C.

About 100 zircons were analysed from BH4; many of these are slightly discordant and have a spread that is indicative of Pb loss. Of the 100 analyses, only eight can be considered inherited and form peaks at *c.* 1.6 and 1.7 Ga, with a single zircon at 1.9 Ga. The remaining 15 zircons define a concordia age of 1449 ± 7 Ma (MSWD = 0.93) (Fig. 2C). This age is somewhat younger than the 1469 ± 6 Ma age presented by Zariņš & Johansson (2009), possibly a consequence of exclusion of a number of zircons with ages around 1500 Ma in this study, which we interpret as being potentially inherited (see electronic appendix).

Table 2. Representative analyses of concordant zircons

SAMPLE & SPOT NAME	U (ppm)	Pb (ppm)	Th/U calc	$^{207}Pb/^{206}Pb$	±2s	$^{207}Pb/^{235}U$	±2s	$^{206}Pb/^{238}U$	±2s	ρ	$^{207}Pb/^{235}U$ age (Ma)	±2s	$^{206}Pb/^{238}U$ age (Ma)	±2s	$^{207}Pb/^{206}Pb$ age (Ma)	±2s	Concordance %
BH1 Knarregård																	
Zircon_sample-012	649	166	0.16	0.092	0.003	3.26	0.30	0.257	0.022	0.95	1472	71	1472	113	1473	55	100
Zircon_sample-015	45	11	0.60	0.092	0.003	3.15	0.13	0.248	0.007	0.67	1445	33	1430	37	1466	60	98
Zircon_sample-016	436	110	0.47	0.091	0.002	3.17	0.10	0.252	0.007	0.79	1451	25	1449	34	1453	39	100
Zircon_sample-026	76	19	0.90	0.092	0.002	3.21	0.22	0.253	0.017	0.95	1460	54	1452	85	1472	41	99
Zircon_sample-027	89	23	0.62	0.092	0.002	3.28	0.10	0.258	0.005	0.63	1477	24	1482	25	1470	45	101
Zircon_sample-033	56	14	0.62	0.092	0.002	3.23	0.12	0.255	0.007	0.71	1465	29	1464	35	1465	50	100
Zircon_sample-036	98	24	0.83	0.092	0.003	3.14	0.26	0.247	0.020	0.94	1442	65	1425	102	1468	53	97
BH3b: Saltuna																	
Zircon_Sample-124	111	27	0.68	0.091	0.002	3.05	0.12	0.243	0.007	0.74	1420	29	1404	35	1444	49	97
Zircon_Sample-138	65	17	0.73	0.093	0.002	3.33	0.17	0.261	0.012	0.89	1489	39	1493	60	1482	44	101
Zircon_Sample-141	92	23	0.55	0.092	0.002	3.14	0.09	0.248	0.005	0.76	1441	22	1426	28	1465	35	97
Zircon_Sample-146	78	19	0.70	0.092	0.003	3.18	0.13	0.250	0.008	0.76	1453	33	1439	42	1475	52	98
Zircon_Sample-156	61	15	0.65	0.091	0.002	3.16	0.14	0.253	0.010	0.88	1448	33	1454	49	1439	39	101
Zircon_Sample-157	114	29	0.68	0.092	0.001	3.16	0.08	0.250	0.005	0.78	1447	19	1438	24	1462	29	98
Zircon_Sample-159	204	52	0.25	0.091	0.003	3.19	0.27	0.254	0.020	0.94	1456	66	1457	104	1454	57	100
BH4 Paridisbakken																	
Zircon_Sample-274	97	24	0.61	0.090	0.003	3.11	0.17	0.250	0.012	0.85	1436	43	1439	61	1431	56	101
Zircon_Sample-277	78	19	0.70	0.091	0.004	3.07	0.20	0.244	0.012	0.74	1424	50	1409	61	1446	85	97
Zircon_Sample-284	328	81	0.74	0.091	0.003	3.08	0.18	0.245	0.012	0.87	1427	44	1415	63	1446	54	98
Zircon_Sample-326	74	18	1.31	0.092	0.002	3.14	0.13	0.248	0.009	0.90	1443	32	1429	48	1463	35	98
Zircon_Sample-341	170	42	0.61	0.092	0.001	3.16	0.09	0.248	0.006	0.83	1447	21	1427	29	1477	29	97
Zircon_Sample-378	79	19	0.55	0.091	0.003	3.07	0.16	0.246	0.010	0.75	1426	41	1416	51	1442	66	98
Zircon_Sample-381	63	16	0.61	0.092	0.002	3.21	0.23	0.252	0.016	0.92	1458	55	1447	84	1475	51	98
BH6: Svaneke																	
Zircon_Sample-059	168	43	0.43	0.092	0.002	3.25	0.20	0.256	0.015	0.93	1469	48	1467	75	1470	42	100
Zircon_Sample-067	137	35	0.39	0.092	0.002	3.24	0.11	0.255	0.007	0.79	1466	27	1466	36	1467	40	100
Zircon_Sample-086	124	31	0.50	0.092	0.002	3.20	0.10	0.251	0.006	0.80	1457	24	1446	33	1472	36	98
Zircon_Sample-090	150	38	0.51	0.092	0.002	3.23	0.11	0.255	0.006	0.66	1464	26	1462	29	1468	47	100
Zircon_Sample-091	89	23	0.65	0.092	0.004	3.28	0.16	0.259	0.007	0.60	1476	37	1485	38	1462	73	102
Zircon_Sample-092	171	42	0.46	0.092	0.002	3.12	0.08	0.247	0.005	0.79	1439	21	1421	27	1464	31	97
Zircon_Sample-093	80	20	1.01	0.092	0.002	3.24	0.10	0.257	0.005	0.63	1467	24	1473	26	1458	46	101
BH8: Almindingen																	
Zircon_Sample-127	516	130	0.64	0.091	0.002	3.18	0.09	0.253	0.005	0.72	1453	23	1452	28	1454	39	100
Zircon_Sample-128	707	177	0.44	0.091	0.001	3.15	0.11	0.251	0.008	0.95	1444	26	1441	42	1448	21	100
Zircon_Sample-131	776	196	0.24	0.091	0.002	3.17	0.11	0.252	0.007	0.83	1451	26	1449	37	1453	36	100
Zircon_Sample-137	1226	303	0.08	0.090	0.002	3.08	0.09	0.247	0.006	0.81	1427	23	1424	31	1432	34	99
Zircon_Sample-141	853	213	0.24	0.090	0.002	3.10	0.17	0.249	0.012	0.88	1433	43	1434	63	1432	50	100
Zircon_Sample-143	558	137	0.76	0.091	0.003	3.08	0.18	0.246	0.012	0.86	1429	45	1417	64	1447	57	98
Zircon_Sample-154	1135	283	0.19	0.090	0.001	3.09	0.11	0.249	0.008	0.88	1430	26	1433	39	1426	31	100
BH11: Vang																	
Zircon_Sample-163	74	18	0.54	0.091	0.005	3.08	0.22	0.244	0.010	0.57	1429	55	1410	52	1457	113	97
Zircon_Sample-164	214	54	0.51	0.092	0.003	3.22	0.18	0.254	0.011	0.75	1461	44	1458	55	1466	72	99
Zircon_Sample-166	110	28	0.55	0.091	0.002	3.19	0.22	0.253	0.016	0.92	1456	53	1456	82	1455	51	100
Zircon_Sample-167	239	59	0.42	0.092	0.002	3.13	0.11	0.248	0.006	0.69	1440	26	1428	30	1459	47	98
Zircon_Sample-169	74	18	0.63	0.092	0.003	3.13	0.11	0.248	0.005	0.54	1439	28	1426	25	1459	58	98
Zircon_Sample-177	110	28	0.76	0.091	0.001	3.17	0.09	0.252	0.006	0.82	1451	21	1447	30	1455	30	99
Zircon_Sample-178	130	33	0.63	0.091	0.002	3.21	0.11	0.254	0.006	0.64	1459	27	1460	29	1457	51	100
BH13: Rønne																	
Zircon_Sample-205	148	38	0.54	0.092	0.004	3.26	0.19	0.256	0.011	0.74	1472	45	1471	56	1472	74	100
Zircon_Sample-214	151	38	0.74	0.092	0.002	3.18	0.07	0.250	0.004	0.69	1452	18	1439	21	1472	32	98
Zircon_Sample-219	74	18	0.54	0.092	0.002	3.17	0.08	0.250	0.004	0.65	1449	19	1438	20	1466	36	98
Zircon_Sample-220	85	22	0.63	0.091	0.001	3.21	0.05	0.255	0.003	0.71	1459	13	1464	15	1450	22	101
Zircon_Sample-221	124	31	0.71	0.092	0.002	3.23	0.14	0.254	0.009	0.81	1464	34	1460	47	1470	49	99
Zircon_Sample-222	164	42	0.78	0.091	0.002	3.20	0.08	0.254	0.003	0.56	1458	18	1460	17	1455	37	100
Zircon_Sample-223	226	58	0.51	0.092	0.002	3.24	0.11	0.255	0.007	0.80	1466	27	1464	36	1468	39	100

SAMPLE & SPOT NAME	U (ppm)	Pb (ppm)	Th/U calc	$^{207}Pb/^{206}Pb$	±2s	$^{207}Pb/^{235}U$	±2s	$^{206}Pb/^{238}U$	±2s	ρ	$^{207}Pb/^{235}U$ age (Ma)	±2s	$^{206}Pb/^{238}U$ age (Ma)	±2s	$^{207}Pb/^{206}Pb$ age (Ma)	±2s	Concordance %
BH15: Naturbornholm																	
Zircon_Sample-244	93	24	0.68	0.092	0.003	3.25	0.15	0.255	0.009	0.80	1469	36	1464	48	1477	52	99
Zircon_Sample-245	132	33	0.63	0.092	0.002	3.21	0.11	0.254	0.007	0.82	1460	28	1459	38	1462	38	100
Zircon_Sample-252	86	22	0.63	0.092	0.002	3.23	0.16	0.253	0.011	0.88	1464	38	1456	57	1474	44	99
Zircon_Sample-253	388	95	0.67	0.091	0.003	3.10	0.18	0.246	0.012	0.85	1432	45	1418	63	1453	59	98
Zircon_Sample-264	99	24	0.55	0.092	0.002	3.11	0.13	0.246	0.010	0.91	1436	33	1418	50	1463	34	97
Zircon_Sample-270	67	16	0.62	0.091	0.004	3.07	0.17	0.244	0.010	0.70	1426	43	1410	49	1451	77	97
Zircon_Sample-271	87	22	0.67	0.092	0.002	3.25	0.22	0.256	0.017	0.94	1469	54	1471	85	1466	46	100
BH21: Hammer																	
Zircon_Sample-284	96	24	0.71	0.092	0.003	3.14	0.15	0.247	0.008	0.70	1443	37	1422	43	1473	65	97
Zircon_Sample-286	144	36	0.56	0.091	0.001	3.14	0.13	0.249	0.010	0.92	1443	32	1436	50	1453	31	99
Zircon_Sample-287	245	63	0.55	0.092	0.002	3.28	0.14	0.258	0.010	0.84	1475	34	1481	49	1467	45	101
Zircon_Sample-292	69	17	0.57	0.092	0.002	3.17	0.13	0.249	0.008	0.77	1449	31	1435	40	1471	49	98
Zircon_Sample-297	568	146	0.56	0.092	0.003	3.26	0.20	0.257	0.013	0.80	1471	48	1477	65	1464	70	101
Zircon_Sample-298	821	205	0.46	0.090	0.002	3.11	0.16	0.250	0.011	0.91	1435	39	1436	59	1432	39	100
Zircon_Sample-303	708	182	0.65	0.091	0.001	3.23	0.13	0.257	0.010	0.96	1464	30	1473	49	1451	21	101
BH24: Mægård																	
Zircon_Sample-326	96	24	0.61	0.091	0.003	3.12	0.16	0.248	0.008	0.67	1439	39	1430	43	1452	71	99
Zircon_Sample-328	86	22	0.70	0.092	0.002	3.23	0.14	0.255	0.008	0.78	1465	33	1463	43	1468	51	100
Zircon_Sample-329	63	15	0.55	0.092	0.002	3.11	0.11	0.246	0.007	0.83	1434	27	1416	37	1461	37	97
Zircon_Sample-331	102	26	0.55	0.091	0.002	3.21	0.13	0.255	0.008	0.82	1459	31	1467	43	1448	44	101
Zircon_Sample-335	103	26	0.51	0.091	0.004	3.14	0.21	0.250	0.011	0.69	1443	51	1437	59	1453	90	99
Zircon_Sample-341	165	43	0.55	0.092	0.002	3.30	0.16	0.259	0.011	0.91	1481	38	1487	59	1472	39	101
Zircon_Sample-342	123	33	0.66	0.092	0.003	3.37	0.16	0.265	0.010	0.81	1499	37	1518	52	1472	54	103
BH27: Rutsker																	
Zircon_sample-008	136	34	0.43	0.090	0.003	3.06	0.22	0.247	0.015	0.86	1424	55	1422	78	1425	70	100
Zircon_sample-011	264	65	0.61	0.091	0.005	3.10	0.29	0.247	0.019	0.81	1433	73	1425	98	1445	105	99
Zircon_sample-012	422	105	0.70	0.091	0.002	3.15	0.19	0.249	0.014	0.92	1444	46	1435	70	1457	44	99
Zircon_sample-020	267	69	0.70	0.092	0.002	3.28	0.17	0.258	0.013	0.94	1475	41	1478	66	1471	34	101
Zircon_Sample-059	90	22	0.51	0.091	0.002	3.13	0.19	0.249	0.013	0.90	1439	46	1432	69	1450	51	99
Zircon_Sample-074	485	121	0.61	0.092	0.001	3.15	0.20	0.249	0.016	0.98	1445	50	1432	81	1465	25	98
Zircon_Sample-087	343	86	0.46	0.091	0.001	3.16	0.15	0.252	0.012	0.97	1448	38	1446	62	1449	22	100

Details on calculation of elemental concentrations, Th/Ucalc, ρ (error correlation) and degree of concordance (concordance %) are given in Frei & Gerdes (2009).

BH6: Svaneke Granite, Listed

This sample is representative of Svaneke Granite (Svaneke Granite type I according to Platou 1970), and was sampled within 10–20 m of a large doleritic dike at Listed. Petrographically, the sample is a relatively coarse-grained granodiorite and displays no apparent foliation in hand specimen although a persistent foliation is evident in outcrop. In thin section, the rock comprises anhedral to subhedral quartz crystals up to 2 mm across and displaying some undulous extinction, anhedral to subhedral plagioclase crystals up to 5 mm in length with albite twinning and some sericitisation and myrmekitic intergrowths along contacts with adjacent quartz. Alkali feldspar occurs as subhedral crystals up to 1 cm in length, displaying cross hatch twinning or perthitic exsolution lamellae. Mafic minerals consist of anhedral crystals of yellow-brown to green-brown pleochroic biotite up to *c.* 4 mm in diameter and showing minor alteration to chlorite, relatively abundant anhedral crystals of titanite up to 1mm in diameter, either present as independent crystals or rimming subhedral opaques. Amphibole occurs as light green to blue green pleochroic anhedral crystals up to 2 mm in diameter. Zircon and apatite are present as accessory phases.

Zircons from this sample are typically subhedral to euhedral prismatic crystals, 100–200 μm long and with width to length ratios of *c.* 1:3. Complex internal magmatic zoning is common, as are darker cores surrounded by thinner brighter rims in BSE images. Representative images are presented in Fig. 2D.

Thirty-one zircons were analysed from this sample. With the exception of a single spot, all analyses are within 10% of being concordant, with the more discordant analyses indicating small amounts of Pb loss. No inherited zircons were identified. Twenty-four zircons fulfilled the requirements of being 97–103% concordant and define a concordia age of 1460 ± 6 Ma (MSWD = 0.57) (Fig. 2D). This age is within error of the three ages presented for Svaneke II (from different localities) by Zariņš & Johansson (2009).

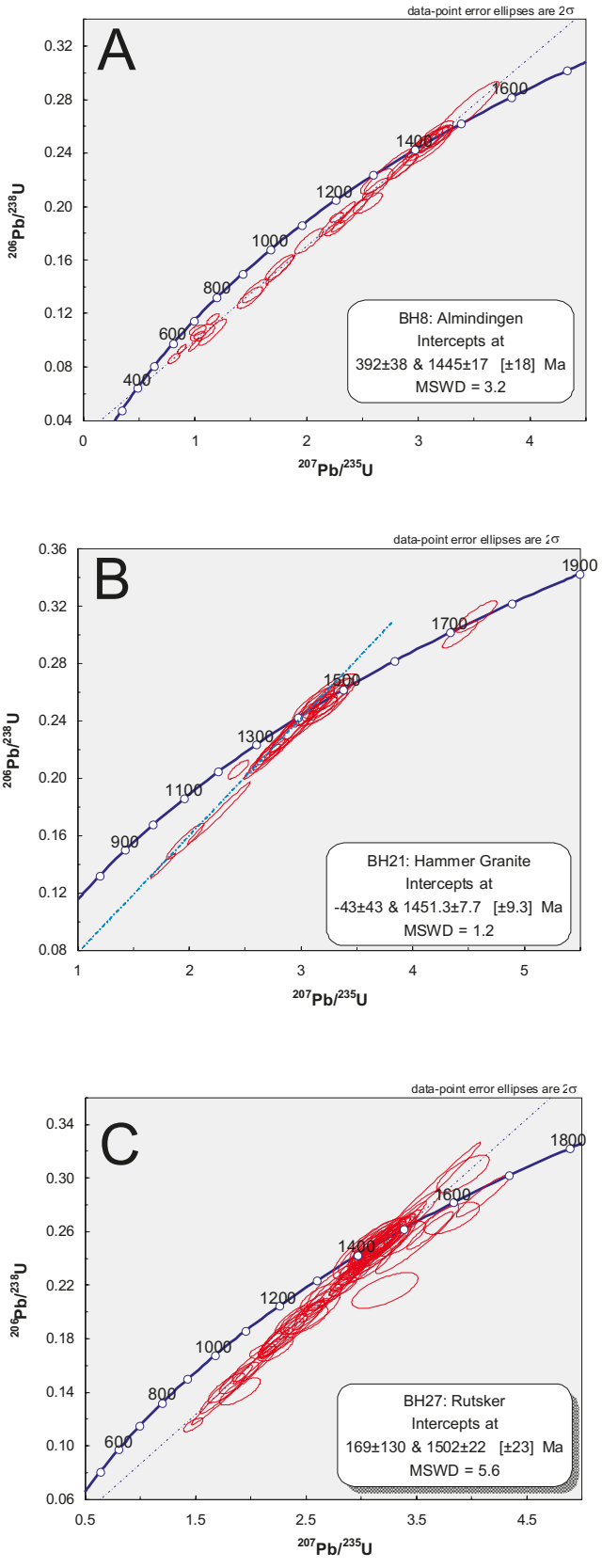

Fig 3. Full concordia plots for three selected samples. These samples show evidence for Palaeozoic to recent Pb loss, as well as rare inherited grains. Intercept ages are calculated using Isoplot (Ludwig 2003) and exclude inherited grains.

BH8: Almindingen Granite

This sample is representative of the Almindingen Granite and is a red, leucocratic, equigranular biotite syenogranite. In thin section, the rock comprises anhedral crystal of quartz up to 4 mm in diameter and displaying undulous extinction, abundant alkali feldspar as anhedral, cross-hatch twinned crystals up to 4 mm in diameter, and subordinate plagioclase as subhedral albite and Carlsbad twinned crystals up to 2 mm in length. Biotite is the dominant mafic phase and is present as anhedral, yellow to brown pleochroic crystals up to 0.5 mm in diameter and often altered to green pleochroic chlorite. Titanite is present as relatively rare anhedral crystals up to 0.5 mm in diameter. Accessory phases include relatively large zircons, possibly allanite, and small subhedral opaque grains up to 0.1 mm in diameter. The rock also displays abundant red iron staining along grain boundaries.

Zircons from this sample are predominantly anhedral to subhedral, stubby crystals *c.* 100–200 μm long and with width to length ratios of *c.* 1:2. Concentric magmatic zoning is common, and many also show patchy zoning; a relatively sharp and thin unzoned rim is developed on many zircons. Sector zoning is evident is a few examples. Representative images of mostly concordant zircons are presented in Fig. 2E.

Thirty-two zircons were analysed from this sample. Many of the zircons have undergone relatively recent Pb loss, possibly associated with the red iron staining observed in thin section, and define an array with an upper intercept age of 1445 ± 7 Ma and a lower intercept of 392 ± 38 Ma (MSWD = 3.2) (Fig. 3A). The discordant zircons do not show any morphological or zoning features to distinguish them from the concordant zircons. The discordant analyses are characterized by relatively high U contents (see appendix) and are therefore likely to be more metamict and more susceptible to Pb loss. The most concordant analyses (better than 97–103% concordant, n = 8) define a concordia age of 1434 ± 8 Ma (MSWD = 1.1) (Fig. 2E). This age is considerably younger than the 1462 ± 5 Ma concordia age presented by Zariņš & Johansson for a sample from the same quarry, although we note that the upper intercept ages for both data sets agree within error. The large degree of Pb loss observed in the sample analysed in this study places the concordia age into question and the upper intercept age of this study or concordia age of Zariņš & Johansson (2009) are preferred here as a crystallization age.

BH11: Vang Granite

This sample is representative of the Vang Granite and was collected from a quarry near the town harbor.

In thin section, the sample is an unfoliated monzogranite and composed of anhedral crystals of quartz up to 1mm in diameter exhibiting undulous extinction and some granophyric intergrowths with alkali feldspar. Plagioclase occurs as subordinate strongly zoned and subhedral crystals up to 5 mm in length, and alkali feldspar is present as abundant relatively fine-grained crystals (*c.* 0.25 mm) with abundant cross hatch twinning. Biotite occurs as yellow-brown to brown pleochroic subhedral crystals up to 0.5 mm in diameter and shows minor alteration to chlorite. Amphibole is present as anhedral yellow-brown to green to blue-green pleochroic crystals up to 2 mm in length. Titanite occurs as a relatively minor phase, typically as generally altered rims on opaque phases, which are present as anhedral crystals up to 1 mm in diameter, commonly forming the cores of clots of mafic minerals (biotite, amphibole, and titanite). Apatite and zircon are present as accessory phases.

Zircons from this sample are subhedral to euhedral stubby to prismatic crystals, typically about 100 μm in length, with width to length ratios of *c.* 1:2. Many are relatively unzoned, although patchy and/or concentric magmatic zoning is also evident. Representative images are presented in Fig. 2F.

Twenty-three zircons were analysed; a few spots are discordant and show evidence for Pb loss, and a single inherited zircon (present as a rounded core with a discordant rim) with an age of 1.9 Ga was identified. The remaining concordant analyses (n = 14) define a concordia age of 1455 ± 8 Ma (MSWD = 0.9) (Fig. 2F). A sample from the same locality investigated in the study of Zariņš & Johansson (2009) yielded a discordant upper intercept age of 1452 ± 22 Ma (MSWD 1.6) and a weighted average $^{207}Pb/^{206}Pb$ age of 1456 ± 8 Ma (MSWD 1.6); nearly all analyses were inversely discordant and therefore a concordia age could not be calculated. The age presented here is in good agreement with, and an improvement on, the previous age determinations.

BH13: Rønne Granite

This is a typical sample of the relatively dark, unfoliated Rønne Granite collected from the Stubbegård quarry. In thin section, this sample is a quartz monzonite comprising anhedral to subhedral crystals of quartz up to 0.5 mm in diameter and displaying minor undulous extinction. Feldspars are present as patchy and strongly zoned, subhedral to anhedral crystals of plagioclase up to 2 mm in length and displaying albite twins and minor sericitisation, and anhedral to subhedral crystals of perthitic or cross-hatch twinned alkali feldspar up to 2 mm in diameter and sometimes occurring as rims on plagioclase crystals (anti-rapakivi texture). Mafic phases include anhedral biotite as yellow-brown to orange-brown to red-brown pleochroic crystals up to 1 mm long and often present as partial clusters of radiating needles. Biotite is subordinate to amphibole, which occurs as abundant anhedral to subhedral green-brown to olive-green pleochroic crystals up to 2 mm in diameter. Many of the amphibole crystals contain a core region consisting of fine-grained complexes of anhedral quartz, opaques and apatite, possibly represented relic cores of clinopyroxene as described by Callisen (1957). Opaque phases occur as subhedral to euhedral crystals up to 0.3 mm in diameter and are commonly surrounded by biotite and hornblende to form the cores of mafic clots. Apatite and zircon are accessory phases.

Zircons from the Rønne Granite sample are generally subhedral to euhedral stubby, prismatic to square crystals displaying generally subtle zoning in the core and relatively bright rims. Crystals are typically 100–150 μm in length with a width to length ratio of 1:2 to 1:3; representative BSE images are presented in Fig. 2G.

Twenty-five zircons were analysed from this sample, and all but four analyses fell within our defined constraints of 97–103% concordance; three analyses show evidence for small amounts of Pb loss, whereas one is slightly older and reversely discordant. Excluding these analyses, the remaining analyses (n = 21) yield a concordia age of 1456 ± 5 Ma (MSWD = 0.9). This age is within error of the 1450 ± 5 Ma age presented by Zariņš & Johansson (2009) on a sample from an adjacent quarry.

BH15: Gneiss, NaturBornholm

This sample comes from the recently excavated 'man-made' exposures at the main car park to NaturBornholm Museum in Aakirkeby, *c.* 400 m north of the fault zone exposed at Klintebakken, and has not been dated in any previous study. Callisen (1934) and Berthelsen (1989) map the region as gneiss, yet in the field the rock bears a strong resemblance to the Svaneke Granite and does not exhibit a well-developed metamorphic fabric. Numerous, metre-wide pegmatite dikes displaying spectacular graphic intergrowths also cut the outcrop. Of all the samples investigated here, this sample is the least fresh. In thin section, the rock is a monzogranite containing quartz as anhedral to subhedral crystals up to 1 mm in diameter and displaying undulous extinction. Plagioclase is present as anhedral to subhedral albite-twinned crystals up to 5 mm in length, is commonly saussiritized, and contains abundant inclusions of fine-grained epidote. Alkali feldspar occurs as sericitised anhedral crystals up top 2 mm in diameter and as perthitic anti-rapakivi rims on plagioclase crystals. Biotite occurs as yellow-brown pleochroic crystals up to 1 mm in length, although

most are altered to green chlorite. Opaques phases occur as subhedral to euhedral crystals up to 0.25 mm in diameter and are commonly rimmed by titanite. Apatite and zircon are accessory phases.

Zircons from this sample are euhedral to subhedral crystals typically 150 μm long, with a width to length ratio of 1:2 to 1:3. Complex zoning is common, but some crystals are relatively homogeneous. Several crystals show metamict cores. Representative BSE images are presented in Fig. 2H.

Nineteen zircons yielded usable analyses from this sample. Several zircons show evidence for Pb loss and were excluded from the data set. A single analysis is inherited with an age of *c.* 1.7 Ga. Only seven remaining zircons fulfil the 97–103% concordance test, possibly a consequence of the alteration observed in thin

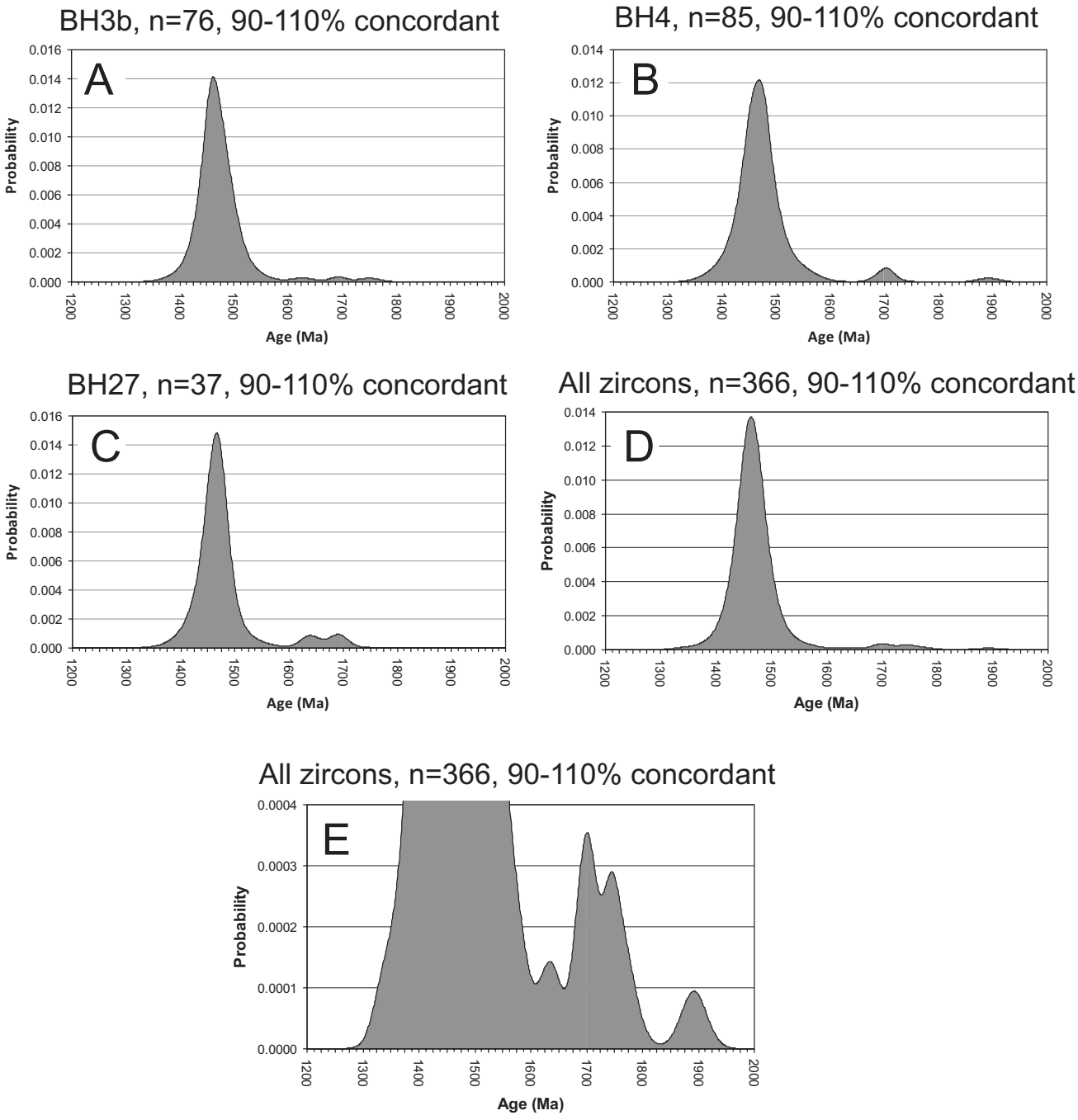

Fig 4: Age probability diagrams for selected samples: A) BH3b (Saltuna gneiss), B) BH4 (Paradisbakke Migmatite), C) BH27 (Rutsker gneiss), D) all zircon analyses from granites and gneisses combined, and E) enlarged view of D illustrating the small peaks in inherited zircons. Diagrams were calculated using AgeDisplay (Sircombe, 2004) and using $^{207}Pb/^{206}Pb$ ages between 90 and 110% concordant, and a bin width of 25 m.y.

section, and combined they yield a concordia age of 1455 ± 13 Ma (MSWD = 0.72) (Fig. 2H).

BH21: Hammer Granite

This sample is a typical example of a weakly foliated variety of the Hammer granite. Petrographically the rock is a syenogranite comprising anhedral crystals of quartz up to 2 mm in diameter and displaying undulous extinction, zoned plagioclase crystals up to 3 mm in length, with both Carlsbad and albite twins and some myrmekitic intergrowths with adjacent quartz, and abundant perthitic alkali feldspar crystals up to 1 cm in length, with some sericitisation. Biotite occurs as subhedral, yellow-green to brown pleochroic crystals up to 0.5 mm in length and sometimes altered to chlorite. Titanite is present as subhedral crystals up to 0.1 mm in diameter in clusters with biotite and relatively rare subhedral opaques up to 0.2 mm in diameter. Amphibole is rare and present as anhedral yellow-brown to green to blue-green pleochroic crystals up to 0.2 mm in diameter. Accessory zircon and apatite are relatively abundant.

Zircons from this sample are typically stubby subhedral to rounded crystals, 100–200 μm long, with width to length ratios of 1:2. Complex magmatic zoning is common. Representative BSE images are given in Fig. 2I.

Twenty-six zircons yielded usable ages from this sample, and of these about half show evidence of Pb loss, trending towards the zero intercept on the concordia diagram (Fig. 3B). Two spots yielded ages indicative of an inherited origin, both at around 1.75 Ga. The remaining analyses define a concordia age of 1458 ± 9 Ma (MSWD = 0.75, n = 9) (Fig. 2I). This age is in excellent agreement with the 1460 ± 7 Ma age presented for a sample from a different location by Zariņš & Johansson (2009).

BH24: Maegård Granite

The Maegård Granite is only exposed in one small, isolated outcrop yet is petrographically and texturally distinct from the other granitoids and gneisses on Bornholm. In hand specimen the rock is relatively fine grained and comprises larger crystals of hornblende and feldspar in a fine-grained matrix. In thin section, the rock is a microgranite and has textures consistent with relatively rapid crystallisation under hypabyssal conditions. It comprises relatively large crystals (phenocrysts) of subhedral, patchily zoned and albite twinned plagioclase up to 5 mm in length and anhedral to subhedral light-green to green pleochroic crystals of amphibole up to 5 mm long in a fine grained microcrystalline mosaical groundmass of anhedral quartz, feldspar, biotite, amphibole and opaques. The amphibole phenocrysts typically contain a core region comprising abundant fine-grained inclusions of quartz and apatite, or weakly green pleochroic clinopyroxene cores. Biotite occurs as rare anhedral red-brown pleochroic phenocrysts up to 2 mm in length. Opaques occur as anhedral to subhedral crystals up to 1 mm in diameter and apatite and zircon are present as accessory phases.

Zircons from this sample are typically anhedral to subhedral crystals around 100–200 μm long and with width to length ratios ranging from 1:2 to 1:3. The crystals are either relatively unzoned or show complex concentric magmatic zoning, with one example of sector zoning observed. Representative images are given in Fig. 2J.

Twenty-nine zircons gave usable results from this sample. Two zircons are highly discordant and preserve evidence for Pb loss. Twenty analyses were 97–103% concordant and combined they yield a concordia age of 1461 ± 7 Ma (Fig. 2J).

BH27: Gneiss, Rutsker

This sample is typical of the more quartz-rich, evolved biotite granitic gneisses that occur throughout Bornholm, and is likely similar to the 'red orthogneisses' described by Zariņš & Johansson (2009). The sample studied here is red, medium grained and equicrystalline and displays a foliation defined by oriented biotite. In thin section, the rock consists of anhedral crystals of quartz up to 0.5 mm in diameter and displaying undulous extinction. Plagioclase is present as relatively rare subhedral, zoned and albite twinned crystals up to 1 mm in length, whereas alkali feldspar is the dominant feldspar and is present as anhedral to subhedral, cross-hatch twinned and perthitic crystals up to 4 mm in length. Biotite defines the foliation and is present as anhedral to subhedral, yellow-brown pleochroic crystals up to 1mm in length, sometimes altered to chlorite. Opaques occur as subhedral to anhedral crystals up to 0.2 mm in diameter and apatite and zircon occur as relatively small accessory phases.

Zircons from this sample are typically subhedral to euhedral prismatic to square 100–150 μm long crystals, with width to length ratios of *c.* 1:2. Complex concentric zoning is common. Representative images are given in Fig. 2K.

Seventy zircons from this sample yielded usable results. Many of these are highly discordant and are indicative of recent Pb loss (see Fig. 3C). Around 10 spots are potentially inherited, normally present as discordant cores to zircons, and yield $^{207}Pb/^{206}Pb$ ages that spread between 1.5 and 1.7 Ga. Twenty-one spots were 97–103% concordant and define a slightly discordant concordia age of 1451 ± 7 Ma (MSWD = 0.16) (Fig. 2K).

Table 3. Results of ^{40}Ar-^{39}Ar step heating experiments on biotite and amphibole from the Rønne Granite

	Laser	Relative Isotopic Abundances										Derived Results					
Lab ID#	Watt	^{40}Ar	±1σ	^{39}Ar	±1σ	^{38}Ar	±1σ	^{37}Ar	±1σ	^{36}Ar	±1σ	$\%^{40}Ar^*$	±1σ	Ca/K	±1σ	Age (Ma)	±1σ
BH13 hornblende																	
1900-01A	2	0.4628	0.0013	0.0054	0.0018	0.0002	0.00001	0.0248	0.0028	0.0006	0.00001	61.29	0.80	9.0853	3.1434	801.6	212.8
1900-01B	3	0.5099	0.0015	0.0114	0.0017	0.0002	0.00001	0.0274	0.0028	0.0003	0.00001	80.34	0.59	4.7260	0.8599	580.6	75.7
1900-01C	4	0.8684	0.0015	0.0229	0.0018	0.0004	0.00001	0.0311	0.0029	0.0003	0.00001	89.60	0.34	2.6634	0.3255	551.6	37.0
1900-01D	5	1.1238	0.0018	0.0467	0.0016	0.0006	0.00001	0.0618	0.0048	0.0003	0.00001	92.34	0.34	2.5941	0.2211	378.3	12.1
1900-01E	6	1.2699	0.0015	0.0873	0.0016	0.0011	0.00001	0.0451	0.0049	0.0003	0.00001	93.14	0.22	1.0141	0.1114	239.9	4.0
1900-01F	7	1.4675	0.0020	0.1015	0.0018	0.0013	0.00002	0.0480	0.0028	0.0003	0.00001	94.22	0.30	0.9272	0.0572	241.0	4.0
1900-01G	10	4.7372	0.0021	0.1275	0.0018	0.0017	0.00002	0.3242	0.0062	0.0009	0.00001	94.90	0.09	4.9850	0.1178	569.4	6.9
1900-01H	13	7.7206	0.0020	0.1186	0.0019	0.0016	0.00001	0.2231	0.0036	0.0008	0.00001	97.24	0.05	3.6888	0.0823	922.0	11.3
1900-01I	16	10.758	0.0021	0.1336	0.0018	0.0017	0.00001	0.0697	0.0032	0.0005	0.00001	98.71	0.04	1.0228	0.0482	1097.6	11.0
1900-01J	19	13.337	0.0023	0.1334	0.0016	0.0018	0.00002	0.1263	0.0051	0.0004	0.00001	99.13	0.03	1.8563	0.0783	1290.8	11.1
1900-01K	22	22.540	0.0027	0.2005	0.0018	0.0029	0.00002	0.4601	0.0039	0.0005	0.00001	99.47	0.02	4.4973	0.0550	1406.7	8.8
1900-01L	25	25.442	0.0026	0.2241	0.0018	0.0033	0.00002	0.5935	0.0042	0.0006	0.00001	99.53	0.02	5.1901	0.0553	1417.1	7.9
1900-01M	27	20.111	0.0026	0.1792	0.0018	0.0025	0.00002	0.4378	0.0038	0.0005	0.00001	99.50	0.02	4.7872	0.0635	1405.2	9.8
1900-01N	29	26.065	0.0026	0.2202	0.0018	0.0033	0.00002	0.7057	0.0065	0.0005	0.00001	99.59	0.02	6.2811	0.0771	1459.8	8.2
1900-01O	31	28.737	0.0028	0.2486	0.0016	0.0037	0.00002	0.8461	0.0080	0.0006	0.00001	99.64	0.02	6.6706	0.0772	1436.6	6.6
1900-01P	33	27.872	0.0026	0.2383	0.0017	0.0036	0.00002	0.8286	0.0044	0.0005	0.00001	99.66	0.02	6.8146	0.0607	1448.6	7.2
1900-01Q	35	24.974	0.0025	0.2177	0.0017	0.0032	0.00002	0.7394	0.0048	0.0005	0.00001	99.66	0.02	6.6565	0.0680	1429.3	7.8
1900-01R	36	11.763	0.0022	0.0999	0.0016	0.0015	0.00001	0.3151	0.0040	0.0002	0.00001	99.65	0.03	6.1796	0.1282	1454.7	16.5
1900-01S-fuse	n.a.	244.11	0.0150	2.0967	0.0019	0.0313	0.00007	7.8954	0.0204	0.0038	0.00002	99.80	0.01	7.3807	0.0202	1445.7	1.0
BH13-biotite																	
1901-01A	2	6.7114	0.0036	0.1801	0.0021	0.0027	0.00002	0.0103	0.0029	0.0021	0.00002	90.81	0.11	0.1121	0.0316	548.6	5.5
1901-01B	3	16.021	0.0042	0.3971	0.0021	0.0055	0.00003	0.0129	0.0031	0.0024	0.00001	95.46	0.04	0.0637	0.0152	612.9	2.7
1901-01C	4	33.713	0.0053	0.6275	0.0022	0.0085	0.00003	0.0184	0.0032	0.0029	0.00002	97.45	0.03	0.0575	0.0099	791.1	2.2
1901-01D	5	62.928	0.0066	0.9152	0.0022	0.0122	0.00004	0.0375	0.0028	0.0035	0.00002	98.34	0.02	0.0802	0.0059	969.4	1.9
1901-01E	6	98.510	0.0079	1.1832	0.0021	0.0154	0.00005	0.0550	0.0033	0.0032	0.00002	99.05	0.01	0.0911	0.0054	1127.6	1.5
1901-01F	7	116.36	0.0093	1.2215	0.0022	0.0157	0.00005	0.0461	0.0032	0.0021	0.00001	99.46	0.01	0.0740	0.0050	1248.8	1.7
1901-01G	8	146.30	0.0101	1.4144	0.0021	0.0179	0.00006	0.0472	0.0032	0.0017	0.00001	99.66	0.01	0.0654	0.0044	1326.8	1.5
1901-01H	9	151.72	0.0101	1.4091	0.0020	0.0178	0.00005	0.0305	0.0033	0.0011	0.00001	99.78	0.01	0.0425	0.0045	1366.2	1.5
1901-01I	10	149.58	0.0121	1.3687	0.0021	0.0173	0.00005	0.0374	0.0034	0.0009	0.00001	99.82	0.01	0.0536	0.0048	1381.0	1.6
1901-01J	11	153.18	0.0111	1.3940	0.0022	0.0174	0.00006	0.0257	0.0035	0.0008	0.00001	99.85	0.01	0.0362	0.0049	1386.6	1.6
1901-01K	14	296.41	0.0151	2.6668	0.0023	0.0332	0.00009	0.0380	0.0034	0.0012	0.00001	99.88	0.01	0.0279	0.0025	1398.0	1.0
1901-01L	16	284.15	0.0180	2.5528	0.0023	0.0318	0.00009	0.0560	0.0034	0.0009	0.00001	99.91	0.01	0.0430	0.0026	1399.7	1.0
1901-01M	18	262.79	0.0150	2.3483	0.0021	0.0293	0.00008	0.1116	0.0034	0.0007	0.00001	99.93	0.01	0.0931	0.0028	1405.1	1.0
1901-01N	20	262.68	0.0160	2.3374	0.0024	0.0290	0.00008	0.0681	0.0031	0.0006	0.00001	99.93	0.01	0.0571	0.0026	1409.3	1.1
1901-01O	22	262.81	0.0160	2.3398	0.0021	0.0291	0.00008	0.0726	0.0027	0.0006	0.00001	99.94	0.01	0.0608	0.0023	1408.9	1.0
1901-01P	24	256.18	0.0170	2.2896	0.0020	0.0283	0.00007	0.0975	0.0032	0.0006	0.00001	99.94	0.01	0.0834	0.0027	1405.1	1.0
1901-01Q	26	242.22	0.0150	2.1652	0.0021	0.0269	0.00008	0.1041	0.0030	0.0005	0.00001	99.94	0.01	0.0943	0.0027	1405.0	1.1
1901-01R	28	227.85	0.0161	2.0368	0.0022	0.0253	0.00007	0.1475	0.0033	0.0005	0.00001	99.94	0.01	0.1420	0.0032	1405.0	1.1
1901-01S	30	211.14	0.0120	1.8840	0.0022	0.0234	0.00006	0.1741	0.0036	0.0005	0.00001	99.94	0.01	0.1811	0.0037	1406.7	1.3
1901-01T	32	185.79	0.0140	1.6577	0.0021	0.0206	0.00006	0.1177	0.0029	0.0004	0.00001	99.94	0.01	0.1392	0.0034	1406.8	1.3
1901-01U	34	157.55	0.0111	1.4081	0.0022	0.0175	0.00005	0.0788	0.0033	0.0003	0.00001	99.94	0.01	0.1096	0.0046	1405.1	1.6
1901-01V	36	128.19	0.0090	1.1489	0.0022	0.0142	0.00004	0.0547	0.0033	0.0002	0.00001	99.95	0.01	0.0933	0.0056	1402.4	2.2

Final step (fusion) sample gas was lost through instrumental error

Separates were irradiated for 40 h in the CLICIT facility of the Oregon State University TRIGA reactor. Sanidine from the Fish Canyon Tuff was used as the neutron fluence monitor with a reference age of 28.172 Ma (Rivera et al., 2011). Nucleogenic production ratios: $(^{36}Ar/^{37}Ar)_{Ca} = 2.646 \pm 0.008 \times 10^{-4}$, $(^{39}Ar/^{37}Ar)_{Ca} = 6.95 \pm 0.09 \times 10^{-4}$, $(^{38}Ar/^{37}Ar)_{Ca} = 0.196 \pm 0.00816 \times 10^{-4}$, $(^{40}Ar/^{39}Ar)_{K} = 7.3 \pm 0.92 \times 10^{-4}$, $(^{38}Ar/^{39}Ar)_{K} = 1.22 \pm 0.0027 \times 10^{-2}$, $(^{36}Ar/^{38}Ar)_{Cl} = 3.2 \times 10^{2}$, $^{37}Ar/^{39}Ar$ to Ca/K = 1.96. Isotopic constants and decay rates: $\lambda(^{40}K_e)$ /yr = 5.8 ± 0.07 x 10^{-11}, $\lambda(^{40}K_{b-})$ /yr = 4.884 ± 0.0495 x 10^{-10}, $\lambda(^{37}Ar)$/d = 1.975 x 10^{-2}, $\lambda(^{39}Ar)$/d = 7.068 x 10^{-6}, $\lambda(^{36}Cl)$/d = 6.308 x 10^{-9}, $(^{40}Ar/^{36}Ar)_{Atm} = 298.56 \pm 0.31$, $(^{40}Ar/^{38}Ar)_{Atm} = 1583.9 \pm 2$, $^{40}K/K_{Total} = 0.01167$.

Inherited zircons and age probability diagrams

Age probability diagrams for three gneiss samples are presented in Fig. 4 A–C. They illustrate that most zircons plot close to the inferred crystallisation age of *c.* 1.45 Ga. Combining all 97–103% concordant zircon analyses from the 11 samples investigated in this study (n = 180) yields a concordia age of 1453 ± 2 Ma (not shown). The age probability diagrams also show that the proportion of inherited zircons is relatively low (generally < 5%). In Fig. 4D, the zircon data (90–110% concordant; n = 366) from all samples are compiled. There is a clear peak at 1460 Ma, representing primary igneous zircon. Additional peaks are identified at 1.63, 1.70, 1.75, and 1.90 Ga (Fig. 4E). Out of the 366 zircons represented in this diagram, only 14 (4%) fall between the age of 1.6 and 1.8 Ga, and 2 fall between the age of 1.8 and 1.9 Ga.

^{40}Ar-^{39}Ar ages

^{40}Ar-^{39}Ar step heating age spectra for amphibole (BH13-hb) and biotite (BH13-bio) separated from Rønne granite sample BH13 are presented in Table 3 and Fig. 5. The amphibole separate yielded a well-defined plateau age of 1446 ± 2 Ma (MSWD = 1.92). The final fusion step for the biotite separate was not measurable due to instrumental issues, and the biotite does not yield a true age plateau in the sense of Fleck *et al.* (1977), i.e. 3 or more contiguous heating steps comprising 50% or more of the ^{39}Ar released and overlapping at the 2 sigma confidence level. Our calculated age for the BH13 biotite is 1405.4 ± 1.3 Ma (MSWD = 0.84) and is based on 7 contiguous steps that overlap at the 2 sigma level and represent just under 40% of the released gas; therefore we are confident that this represents an accurate age. Both these ages are significantly younger than the U-Pb zircon age for the same sample of 1456 ± 5 Ma.

Rb-Sr age

The amphibole, biotite and feldspar separates from Rønne Granite sample BH13 yield a poorly-defined 3-point errorchron, giving an age of 1378 ± 110 Ma with a high MSWD; addition of the whole rock sample improves the error on the age (1372 ± 33 Ma), yet the MSWD remains high suggesting disequilibrium or alteration of some mineral phases (Table 4). The Rb-Sr age in this study is primarily defined by the highly radiogenic biotite separate (^{87}Sr/^{86}Sr = 3.94) and various 2-point isochrons can be calculated using different minerals or by assuming an initial ^{87}Sr/^{86}Sr within geologically reasonable limits. These calculations all result in ages of around 1370 ± 14 Ma.

Discussion

Zircon ages

The U-Pb zircon ages presented here confirm the results of Zariņš & Johansson (2009) and indicate that all granitic magmatism on Bornholm took place over a relatively restricted period at 1.45 Ga. This event includes the previously undated Maegård Granite that, despite its textural contrasts with other Bornholm felsic basement lithologies, was emplaced during the same event. There is no evidence for an older and younger suite of granitoids as proposed by Micheelsen

Table 4: Rb-Sr isotope data for mineral separates and whole rock powder for sample BH13 from the Rønne Granite

Sample	^{87}Rb/^{86}Sr	2SE%	^{87}Sr/^{86}Sr	2SE%	
BH13 Biotite	164.3	0.012	3.9432	0.0006	
BH13 Amphibole	2.995	0.476	0.77779	0.0011	
BH13 Feldspar	2.18	0.032	0.74913	0.0011	
BH13 Whole rock	2.356	0.023	0.75695	0.0014	
Age calculations	**Age (Ma)**	**error (Ma)**	**^{87}Sr/^{86}Sr$_{(i)}$**	**error**	**MSWD**
Bio+Amp+Fsp+whole rock	1372	33	0.712	0.016	516
Bio+Amp+Fsp	1372	110	0.713	0.082	1032
Bio+whole rock	1372	14	0.71059	0.00065	na
Bio+Amp	1369	14	0.719	0.00083	na
Bio+Fsp	1374	14	0.70618	0.0006	na
Bio model	1375	13	0.703		na
Bio model	1364	13	0.73		na

Bio = biotite, Amp = amphibole, Fsp = feldspar. na = not applicable. Ages were calculated in Isoplot (Ludwig 2003) assuming reproducibilities of 1% for ^{87}Rb/^{86}Sr and 0.003% for ^{87}Sr/^{86}Sr (Waight *et al.* 2002a,b). The model ages are calculated assuming initial ^{87}Sr/^{86}Sr ratios of 0.703 and 0.730. Errors on measured Rb/Sr and ^{87}Sr/^{86}Sr are based on in-run statistics.

(1961) and Berthelsen (1989). Furthermore, our zircon dating of additional gneissic lithologies to those studied by Zariņš & Johansson (2009) has failed to identify any older 1.8 Ga basement lithologies on Bornholm, as observed to the north in southern Sweden in the Blekinge Province (e.g. Johansson & Larsen, 1989; Johansson *et al.* 2006). The relatively low abundance of inherited zircons in the Bornholm granitoids suggests that basement of this age was not significantly involved as a source region or contaminant during granitic magmatism. Callisen (1956), Platou (1970) and Friis (1996) described occurrences of high-grade metasedimentary inclusions (muscovite-bearing quartz-rich gneisses, quartzite, garnet-epidote and wollastonite skarns) between Gudhjem and Svaneke along the north coast of Bornholm, in Rønne Granite, Vang Granite, and near Paradisbakkerne, that potentially represent older sediments. However, without more detailed chronological investigations their provenance and relationship to older basement lithologies elsewhere in Scandinavia remains unknown.

A geological history on Bornholm where the gneissic rocks represent older metamorphic basement and the less deformed to undeformed granitoids represent younger intrusions is not confirmed by the available modern geochronological data. Instead, there is no statistical difference in age between essentially undeformed granitoids (e.g. Rønne and Maegård),

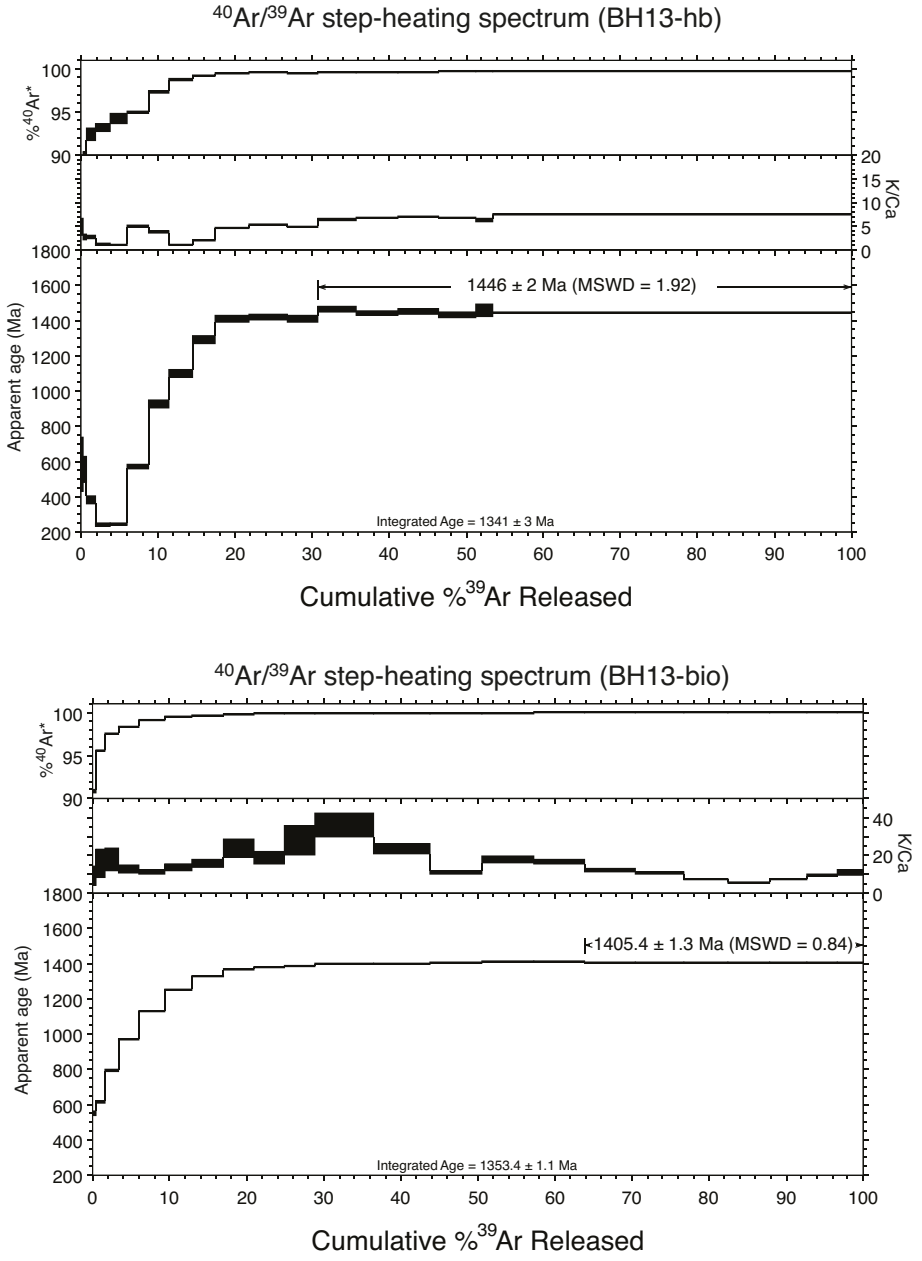

Fig 5. ^{40}Ar-^{39}Ar laser step heating age spectra for amphibole (BH13-hb) and biotite (BH13-bio) from the Rønne Granite. Boxes represent individual steps and two sigma errors.

more deformed granitoids such as Svaneke, and gneisses with clear metamorphic fabrics such as BH1 from Knarregård. Therefore, magmatism, deformation, and metamorphism must have occurred largely 'simultaneously' at *c.* 1.45 Ga. We note however that these deformational and magmatic events may have occurred over a period of up to 20 Ma given the errors of the geochronological techniques used here. Petrographically and geochemically the gneisses and granitoids resemble each other and can be broadly grouped into either relatively felsic biotite granitoids/gneisses (e.g. Hammer Granite, Almindingen Granite, Rutsker gneiss) or more intermediate amphibole-bearing lithologies (e.g. Rønne Granite, Vang Granite, Knarregård gneiss) (e.g. Berthelsen 1989; Waight & Bogdanova unpublished data). It is therefore likely that the basement lithologies on Bornholm represent a multiphase magmatic event that occurred in part contemporaneously with deformation. The distinction between the gneiss and granitoid on Bornholm is therefore primarily a consequence of varying degrees of fabric development and does not represent different intrusive events. In fact, many of the basement lithologies defined as granitoid also show signs of fabric development, likely a consequence of deformation at mid-lower crustal conditions during the later stages of crystallization and/or immediately post-solidus. Fabric development likely represents deformation of slightly older intrusions (either at close to solidus or subsolidus conditions) during emplacement of slightly younger plutons. Similar arguments have been presented based on detailed structural, textural, and magnetic susceptibility studies of the contemporaneous Karlshamn pluton in southern Sweden (Čečys & Benn 2007).

Pb loss

A number of samples show evidence for substantial Palaeozoic to recent Pb loss. The sample most affected by Pb loss is BH8 from the Almindingen Granite. This sample was collected from a large loose block located near to a crosscutting, NW-trending mugearite (kullaite) dike (Jensen 1988; Obst 2000). Holm *et al.* (2010) have suggested that the NW-trending dikes on Bornholm are relatively young (*c.* 300 Ma). This age is close to the age of Pb loss at Almindingen as defined by the lower intercept age of 392 ± 38 Ma (Fig. 3A) and we suggest that Pb loss in this sample was a result of thermal disturbance during dike emplacement. However, it is also interesting to note that in contrast sample BH3b collected *c.* 50 m from the Kelseå dike (1326 Ma; Holm *et al.* 2010) and BH6 collected within 10-20 m of the Listed Dike (950 Ma; Holm *et al.* 2010) show limited evidence for Pb loss, despite the relatively large size of the nearby dikes. Furthermore, the sample of Almindingen Granite analysed by Zariņš & Johansson (2009) was collected from the same quarry as BH8 yet exhibits little evidence for Pb loss.

Cooling and uplift

The wide range in ages (1.46–1.37 Ga) recorded using different isotope systems and mineral phases within a single sample (BH13) from the Rønne Granite is consistent with the wide scatter of ages that have been presented using different isotopic systems on Bornholm and elsewhere in southern Scandinavia (see Obst *et al.* 2004 for a summary). For example, the various two-point biotite ages calculated in this study (Table 4) of *c.* 1370 Ma are in good agreement with unpublished Rb-Sr mineral-whole rock ages for the Rønne Granite (1372 ± 9 Ma) and Vang Granite (1347 ± 12 Ma) (Tschernoster 2000 in Obst *et al.* 2004). These ages are also in broad agreement with mineral - whole rock ages for various intrusions on Bornholm and elsewhere that range between 1240 and 1380 Ma and are clearly younger than U-Pb zircon ages on the same lithologies (see Obst 2004). As the ages from different isotope systems presented in this study are based on a single sample, we can assume that this range in temperatures reflects variations in the closure temperatures for different minerals and different isotopic systems and therefore use this information to place constraints on the cooling and uplift history of Bornholm in the Proterozoic.

Sources for closure temperature estimates used here are taken in part from the compilations made by Villa (1998) and Willigers *et al.* (2001). Assumed closure temperatures used are: U-Pb in zircon = 900+°C (Lee *et al.* 1997); K-Ar in amphibole = 600°C (Kamber *et al.* 1995; Villa 1998); K-Ar in biotite = 450°C (Villa 1998); and Rb-Sr in biotite = 300°C (Dodson 1973), although we note that even lower closure temperatures for Rb-Sr in biotite (<200°C) have been suggested (e.g. Brabander & Giletti 1995). We use the biotite-whole rock 2-point isochron as a best estimate of the age at which biotite closed to Sr isotopic diffusion with the whole rock composition. Use of any of the other 2-point isochron ages has little consequence for the results, and we discuss the possible origins of the failure of the combined mineral and whole rock data to form an isochron below. Combined, the closure temperatures and ages presented above define a potential cooling curve for the Rønne Granite, and by inference, for the entire basement block of Bornholm (Fig. 6). Combining the geochronological data with assumed closure temperatures presented above (solid symbols in Fig. 6) suggests a period of relatively rapid cooling of at least 30°C per million years immediately following

emplacement of the granitoid and crystallisation of zircon and down to the closure of the K-Ar system in amphibole at *c.* 600°C. This initial period of rapid cooling was followed by cooling from *c.* 600°C at a rate that was around an order of magnitude slower (4°C per million years) until closure of the Sr system in biotite at around 300°C.

We note that potential errors in the decay constant of ^{40}K have not been taken into account in our age calculations. Recent studies have highlighted potential problems caused by uncertainties in decay constants when comparing ages determined using different decay schemes. In particular, these uncertainties result in a potential bias such that $^{206}Pb/^{238}U$ ages can be up to 0.5% older than ^{40}Ar-^{39}Ar ages in the same sample for rocks of approximately the same age as those on Bornholm (Renne *et al*. 2010). Taking this into account, it is thus possible that the U-Pb zircon and ^{40}Ar-^{39}Ar amphibole age on the Rønne Granite are effectively the same within analytical error, as illustrated in Fig. 6. However, it is important to note that the differences between the biotite and amphibole ^{40}Ar-^{39}Ar age determinations are unaffected by decay constant complications and therefore this age difference is real and must be a consequent of different closure temperatures.

Zariņš & Johansson (2009) report U-Pb ages for titanite from a number of Bornholm basement samples, although not specifically from the Rønne Granite where titanite is absent to sparse. Concordia ages for titanite range from 1452 ± 11 Ma (red orthogneiss at Gudhjem) to 1437 ± 18 Ma (Vang) (average = 1445 Ma, n=5) and are generally within error of, or slightly younger than, the U-Pb zircon age from the same samples. Closure temperatures for U-Pb in titanite are somewhat lower than for zircon and estimated at 670°C by Dahl (1997). As shown in Fig. 6, this lower closure temperature is consistent with the U-Pb ages and Ar age in amphibole representing isotopic closure during relatively rapid cooling following emplacement and crystallisation of the granitoids.

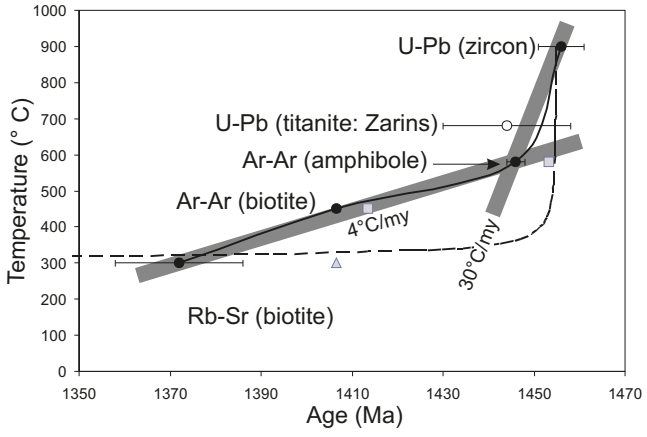

Fig. 6. Cooling history for the Rønne Granite (see text for discussion). Solid line represents a cooling curve predicted using recent literature values for closure temperatures (solid symbols). The open circle represents U-Pb ages on titanite from Zariņš & Johansson (2009). The dashed line represents a cooling curve modelled using the one dimensional heat conduction equation (e.g. Stuŵe 2007) assuming a temperature drop from 900°C to 300°C at emplacement depths of 10 km and assuming a thermal conductivity constant of $10^{-6}m^2s^{-1}$. The grey squares represent the effect of increasing the Ar age for amphibole and biotite by 0.5% to account for potential discrepancies between the decay constants for U-Pb and K-Ar. The grey triangle represents the Ar biotite age assuming a lower closure temperature of 300°C.

Emplacement conditions of the Rønne Granite are estimated at *c.* 750°C and 3.1 kb (around 10 km) using Al-in-amphibole contents and calculated using the spreadsheet of Anderson *et al.* (2008), and using the plagioclase-hornblende geothermobarometers of Blundy & Holland (1990) and Andersen & Smith (1995) (Waight, unpublished data). These data suggest that the initial period of cooling was associated with the initial emplacement and crystallisation of the granitoids. All deformation of the granitoids and gneisses must also have occurred during this period and at these pressure-temperature conditions, based on the overlap within error of the U-Pb zircon ages of deformed and undeformed lithologies.

Using the relatively recent closure temperatures from the literature discussed previously, the initial period of rapid cooling subsequent to emplacement was followed by cooling from *c.* 600–750°C (closure temperature for Ar in amphibole and crystallisation temperature of the granitoids). This occurred at a rate that was around an order of magnitude slower (4°C per million years) until closure of the Sr system in biotite at around 300°C. Assuming a geothermal gradient of 30°C/km, this is equivalent to an uplift rate of *c.* 0.1 mm/yr. Such relatively slow cooling rates are typical for regions of post-orogenic exhumation by erosion in the Precambrian and contrast markedly with rapid tectonic uplift of mid-deep crustal lithologies seen in Phanerozoic orogens (see Willigers *et al.* 2002 for a review and discussion). However, as discussed below, this apparent cooling curve should be viewed with caution.

Heat loss following emplacement of plutons will be dominated by conduction to the surface, and this can be modelled using the one dimensional diffusion or heat conduction equation (e.g. Stuŵe 2007). Such a curve illustrating cooling from 900°C to 300°C at emplacement depths of 10 km is shown as a dashed line in Fig. 6. This model predicts an initially relatively rapid drop in temperature over a period of < 20 Ma to around 350°C followed by near isothermal conditions

and is significantly different from the apparent cooling rate as defined primarily by the Ar age for biotite. The exact closure temperature for the Ar system in biotite is unresolved (e.g. Reno *et al.* 2012) and may be as low as *c.* 300°C in slowly cooled, fluid-bearing systems (Harrison *et al.* 1985). Allaz *et al.* (2011) have shown that minor chloritisation of biotite during uplift, retrograde metamorphism, or deuteric alteration can have important consequences for resetting Ar isotope systematic in biotite, and alteration of biotite to chlorite is common in the Bornholm granitoids. Use of this lower closure temperature places the ^{40}Ar-^{39}Ar biotite age on the cooling curve predicted by one-dimensional heat conduction. Furthermore, a potential 0.5% increase in the ^{40}Ar-^{39}Ar amphibole age to account for potential calibration issues between decay constants of the U-Pb and K-Ar systems moves the amphibole age onto the theoretical cooling curve. A similar 0.5% increase in the biotite ^{40}Ar-^{39}Ar age will just shift the age along the cooling curve. As the slope of the cooling curves are primarily defined by the Ar age on biotite, the 'true' cooling history of the Rønne Granite may lie anywhere between the two extremes presented in Fig. 6. However, as most Rb-Sr biotite ages from Bornholm are significantly younger than U-Pb zircon ages (see summary in Obst *et al.* 2004), a relatively slow cooling rate is implied. These results illustrate the complications involved in constructing cooling curves; however the clear differences between U-Pb systematics in zircon (Zariņš & Johansson 2009; this study) and Rb-Sr ages based on mica (Obst *et al.* 2004; this study) indicate that the latter cannot be used to define intrusion ages for the Bornholm granitoids. Furthermore, the Rb-Sr ages based on biotite in the granitoids also suggest that the approximate ambient temperature of the crust at the time of onset of the oldest mafic dike activity on Bornholm at *c.* 1330 Ma (Holm *et al.* 2010) was around 300°C.

Apatite fission track data from the Hammer Granite indicate that the basement on Bornholm was last uplifted through 100°C (*c.* 3 km depth assuming 30°C/km) at around 260 Ma (Hansen 1995) although the basement granites were likely exposed prior to this to provide sources for sediments such as the Cambrian Nexø sandstone. It is therefore clear from the geochronological data presented here that the crust in Bornholm has remained relatively stable for a prolonged period from *c.* 1350 Ma through to the modern day, and has not been affected significantly by subsequent tectonic events elsewhere in the region such as the Sveconorwegian or Caledonian orogenies.

The differing closure temperatures of mineral systems can also potentially explain the high MSWD for the combined mineral and whole rock Rb-Sr data for sample BH13, which clearly indicate that the sample is disturbed or that some other geological or analytical factor is involved in causing disequilibrium between coexisting phases. Brabander & Giletti (1995) have shown that the estimated closure temperatures for Sr isotopes in hornblende (*c.* 625–700° C) are higher than for Na-rich feldspar (*c.* 500° C) which are in turn higher than those estimated for biotite (300° C or lower). Variations in closure temperature, as well as the potential effects of radiogenic ingrowth during cooling, will result in variations in ages and initial isotope compositions, and therefore statistically perfect isochrons will be unlikely to be preserved.

Correlation

As stated above, the felsic basement lithologies of Bornholm were emplaced during a relatively restricted, multi-phase event at 1.45 Ga. Correlations of these rocks with intrusions of similar ages throughout southern Scandinavia as well as Eastern Europe and southwards towards Poland (drill hole G-14) have been summarised by Obst *et al.* (2004) and Zariņš & Johansson (2009), and readers are referred to those works for a more comprehensive summary of previous geochronological studies. A magmatic event at 1.45 Ga is evident throughout the western Eastern European craton and has been referred to as the Danolopolian orogeny by Bogdanova *et al.* (2008). The magmatism is linked to deformation and shearing along large-scale E–W and NW–SE trending shear zones, which commonly accommodate syntectonic granitoids. It is likely that the basement rocks of Bornholm were also emplaced into such a shear zone. Bogdanova (2001) suggested that the Danolopolian event was the result of collision between Baltica and another continental block, potentially Amazonia or another South American crustal block.

The granitoids of Bornholm and southern Sweden (e.g. Stenshuvud and Tåghusa) share chemical characteristics that suggest classification as A-type or 'within-plate granites' according to the tectonic discrimination diagrams of Pearce *et al.* (1984) (e.g. Čečys *et al.* 2002; Obst *et al.* 2004; Waight & Bogdanova, unpublished data). Within-plate granitoids are typically considered to be anorogenic, in the sense that they are not associated with crustal collision or subduction processes. Within-plate granitoids form in extensional, rift-type environments such as observed in the East African Rift and in the Oslo Rift; in post-collisional settings; or are associated with plume activity (Pearce *et al.* 1984; Eby 1990). Use of the term anorogenic can be misleading, however, as these tectonic settings may also be structurally active, as suggested by Čečys & Benn (2007), and as also indicated by the apparently contemporaneous nature of deformation and magma-

tism on Bornholm as indicated by our U-Pb geochronological results from Bornholm. If deformation is not purely extensional, but also includes a component of transtensional or transpressional shearing, then synmagmatic deformation is likely. Moreover, this may also provide a mechanism for creating space in the crust for the upwards migration and emplacement of granitoid magmas (e.g. Hutton *et al.* 1990; Hutton & Reavy 1992). More detailed structural studies are needed to further clarify the intrusive/deformational environment on Bornholm, and these may well be hampered by the limited exposure available.

Comparison between SIMS and LA-ICPMS

As a final note, the duplication of age determinations on samples from the same lithologies and, in some cases, from similar locations, in this study using LA-ICPMS and in the study of Zariņš & Johansson (2009) using ion microprobe, offers a perfect opportunity to compare the two techniques. In most cases, ages obtained on the same lithologies and/or localities in the two studies agree closely or within error, and the errors obtained on the ages (*c.* 0.5% absolute) are similar for both techniques. In those cases where the ages do not agree, the discrepancies can generally be explained by close examination of the data and as in, for example, the Almindingen Granite can be explained using well-established complications in the U-Pb zircon system such as Pb loss. The example of the Almindingen granite also illustrates the role that sample selection plays, with two samples from effectively the same locality displaying significant differences in the degree of disturbance of the zircons. A clear advantage of the LA-ICPMS method is the rapid throughput of samples and production of data with each analysis taking only a few minutes at most, compared with around 20 minutes for a typical SIMS analysis. All U-Pb data in this study were produced over an analytical session of two days, and all analyses (including standards) were run automatically following pre-programming of the points to be analysed. The main time factor involved in LA-ICPMS analysis (and SIMS for that matter) is thus sample preparation and characterisation. This rapid throughput is especially useful for provenance studies and large-scale geochronological campaigns. Advantages of the SIMS method are potentially smaller spot-sizes (down to 10 μm) although both methods typically use similar spot-sizes, and that it is much less destructive. SIMS typically evacuates pits of around 5 μm, thus making it the preferred method for valuable and unique samples such as meteorites, and leaving zircon mounts more amenable to subsequent investigations such as for Hf isotopic composition. A disadvantage to both techniques is the error on obtained ages, which are limited to around 1–1.5% absolute, in this case equating to *c.* ± 10 Ma on a 1450 Ma sample. In both this study and that of Zariņš & Johansson (2009), we were unable to make age distinctions between different intrusions. Determining the relative ages of the intrusives must therefore rely on observations of cross-cutting relationships in the field (e.g. Callisen 1934; Micheelsen 1961; Berthelsen 1989 and references therein), potentially coupled with more precise absolute age determinations through application of more time-consuming and arduous geochronological techniques, such as single-zircon and chemical abrasion TIMS methods (e.g. Mattinson 2005).

Conclusions

New LA-ICPMS U-Pb zircon ages for 11 samples of granitoid and gneiss from the Danish island of Bornholm indicate that the felsic basement was formed at 1455 ± 10 Ma. At the levels of error available using this technique no age distinction can be made between deformed gneissic samples and less deformed or undeformed granitoids, indicating that magmatism and deformation on Bornholm occurred within this relatively restricted timeframe. Analyses of several gneissic samples, combined with the previous analyses of Zariņš & Johansson (2009), have failed to identify any outcrops of 1.8 Ga basement on Bornholm. No evidence for resetting during later large-scale tectonic events has been found.

More detailed studies of a number of samples, involving analyses of up to 100 zircons from each, indicate that the degree of zircon inheritance in the Bornholm granitoids and gneisses is low (<4%), with broad peaks identified at *c.* 1.6–1.8 Ga and 1.8–1.9 Ga. These results indicate that older basement components did not play a large role as sources or contaminants during magma genesis.

Chronological studies of a single sample of the Rønne Granite using U-Pb in zircon, ^{40}Ar-^{39}Ar in amphibole and biotite, and Rb-Sr in biotite, suggest a cooling history for Bornholm that was initially relatively fast (*c.* 30° C per million years), likely indicative of the period of magma emplacement, crystallization and post-emplacement cooling. This was followed by a longer period of slower cooling or isothermic conditions, and the region appears to have first cooled through the closure temperature of Sr isotopes in biotite (*c.* 300°C) 70–90 Ma after pluton emplacement. More detailed constraints on the post-emplacement cooling history are complicated by precise definition of the closure temperature of the Ar system in biotite.

Acknowledgments

We would like to thank Peter Venslev for assistance with crushing and for excellent mineral separation work, without which this work would probably have never happened. Barry Reno is thanked for discussions on closure temperatures and cooling curves, and for providing a spreadsheet for calculating thermal conductive cooling. Anne and Clara-Marie Dyreborg are thanked for their assistance during fieldwork. The manuscript benefitted from the constructive and clarifying comments of Henrik Friis and Svetlana Bogdanova. This study was funded by a grant from the Carlsberg Foundation. QUADLAB is supported by the Villum Foundation.

References

Åberg, G. 1988: Middle Proterozoic anorogenic magmatism in Sweden and worldwide. Lithos 21, 279–289.

Allaz , J., Engi, M., Berger, A. & Villa, I.M. 2011: The effects of retrograde reactions and of diffusion on ^{40}Ar-^{39}Ar ages of micas. Journal of Petrology 52, 691–716.

Anderson, J.L. & Smith, D.R. 1995: The effect of temperature and oxygen fugacity on Al-in-hornblende barometry. American Mineralogist 80, 549–559.

Anderson, J.L., Barth, A.P., Wooden, J.L. & Mazdab, F. 2008: Thermometers and thermobarometers in granitic systems. Reviews in Mineralogy and Geochemistry 69, 121–142.

Blundy, J. D. & Holland, T. J. B. 1990: Calcic amphibole equilibria and a new amphibole-plagioclase geothermometer. Contributions to Mineralogy and Petrology 104, 208–224.

Berthelsen, A. 1989: Bornholms geologi III: Grundfjeldet. Varv 1989(1), 1–40.

Bogdanova, S. 2001: Tectonic settings of 1.65–1.4 Ga AMCG Magmatism in the Western East European Craton (Western Baltica). Journal of Conference Abstracts, EUG XI, 6, 769 only.

Bogdanova, S.V., Bingen, B., Gorbatschev, R., Kheraskova, T.N., Kozlov, V.I., Puchkov, V.N. & Volozh, Y.A. 2008: The East European Craton (Baltica) before and during the assembly of Rodinia. Precambrian Research 160, 23–45.

Brabander, D.J. & Giletti, B.J. 1995: Strontium diffusion kinetics in amphiboles and significance to thermal history determinations. Geochimica et Cosmochimica Acta 59, 2223–2238.

Brumm, A., Jensen, G.M., van der Bergh, G.D., Morwood, M.J., Kurniawan, I., Aziz, F. & Storey, M. 2010: Hominins on Flores, Indonesia, by one million years ago. Nature 464, 748–752.

Callisen, K. 1934: Das Grundgebirge von Bornholm. Danmarks Geologiske Undersøgelse II Række 50, 266 pp.

Callisen, K. 1956: Fragmenter og spor efter bjergarter ældre end graniten på Bornholm. Meddelelser fra Dansk Geologisk Forening 13, 158–173.

Callisen, K. 1957: Hornblende with pyroxene core in the Rønne granite. Meddelelser fra Dansk Geologisk Forening 13, 236–237.

Čečys, A. & Benn, K. 2007: Emplacement and deformation of the c. 1.45 Ga Karlshamn granitoid pluton, southeastern Sweden, during ENE–WSW Danopolonian shortening. International Journal of Earth Sciences 96, 397–414.

Čečys, A., Bogdanova, S., Jansson, C., Bibikova, E. & Kornfält, K.-A., 2002: The Stenshuvud and Tåghusa granitoids: new representatives of Mesoproterozoic magmatism in southern Sweden. Geologiska Föreningens i Stockholm Förhandlingar 124, 149–162.

Dahl, P.S. 1997: A crystal-chemical basis for Pb retention and fission tracks annealing systematics in U-bearing minerals, with implications for geochronology. Earth and Planetary Science Letters 150, 277–290.

Dodson, M.H. 1973: Closure temperatures in cooling geochronological and petrological systems. Contributions to Mineralogy and Petrology 40, 259–274.

Eby, G.N. 1990: The A-type granitoids: A review of their occurrence and chemical characteristics and speculations on their petrogenesis. Lithos 26, 115–134.

Fleck, R.J., Sutter, J.F. & Elliot, D.H. 1977: Interpretation of discordant ^{40}Ar-^{39}Ar age-spectra of Mesozoic tholeiites from Antarctica. Geochimica et Cosmochimica Acta 41, 15–32.

Frei, D. & Gerdes, A. 2009: Precise and accurate in situ U–Pb dating of zircon with high sample throughput by automated LA-SF-ICPMS. Chemical Geology 261, 261–270.

Friis, H. 1996: A quartzite inclusion in the Rønne Granite - the first Danish sediment. Bulletin of the Geological Society of Denmark 43, 4–8.

Gerdes, A. & Zeh, A. 2006: Combined U-Pb and Hf isotopes LA-(MC)-ICP-MS analyses of detrital zircons: comparison with SHRIMP and new constraints for the provenance and age of an Armorican metasediment in Central Germany. Earth and Planetary Science Letters 249, 47–61.

Gorbatschev, R. & Bogdanova, S. 1993: Frontiers in the Baltic Shield. Precambrian Research 64, 3–21.

Graversen, O. 2009: Structural analysis of superposed fault systems of the Bornholm horst block, Tornquist Zone, Denmark. Bulletin of the Geological Society of Denmark 57, 25–49.

Gravesen, P. 1996: Geologisk set – Bornholm. Geografforlaget: Brenderup, 208 pp.

Hansen, K. 1995: Fennoscandian Border zone: thermal and tectonic history of a tuffaceous sandstone and granite from fission track analysis, Bornholm, Denmark. Tectonophysics 244, 153–160.

Harrison, T.M., Duncan, I., & McDougall, I. 1985: Diffusion of ^{40}Ar in biotite: Temperature, pressure and compositional effects. Geochimica et Cosmochimica Acta 49, 2461–2468.

Holm, P.M., Pedersen, L.E. & Højsteen, B. 2010: Geochemistry and petrology of mafic Proterozoic and Permian dykes on Bornholm, Denmark: Four episodes of magmatism on the margin of the Baltic Shield. Bulletin of the Geological Society of Denmark 58, 35–65.

Hutton, D.H.W. & Reavy, R.J. 1992: Strike-slip tectonics and granite petrogenesis. Tectonics 11, 960–967.

Hutton, D.H.W., Dempster, T.J., Brown, P.E. & Becker, S.D. 1990: A new mechanism of granite emplacement – intrusion in active extensional shear zones. Nature 343, 452–455.

Jensen, A. 1988: The Bjergebakke dyke - a kullaite from Bornholm. Bulletin of the Geological Society of Denmark 37, 123–140.

Johansson, Å. & Larsen, O. 1989: Radiometric age determinations and Precambrian chronology of Blekinge, southern Sweden. Geologiska Föreningens i Stockholm Förhandlingar 111, 35–50.

Johansson, Å., Bogdanova, S. & Čecys, A., 2006: A revised geochronology for the Blekinge Province, southern Sweden. GFF 128, 287–302.

Kamber, B.S., Kramers, J.D., Napier, R., Cliff, R.A. & Rollinson, H.R. 1995: The triangle shear zone, Zimbabwe, revisited: new data document and important event at 2.0 Ga in the Limpopo Belt. Precambrian Research 70, 191–213.

Kornfält, K-A. 1993: U-Pb zircon ages of three granite samples from Blekinge County, south-eastern Sweden. Sveriges Geologiske Undersøgelse Serie C 823, 17–23.

Kornfält, K-A. 1996: U-Pb zircon ages of six granite samples from Blekinge County, southeastern Sweden. Sveriges Geologiske Undersøgelse Serie C 828, 15–31.

Larsen, O. 1971: K/Ar Age determinations from the Precambrian of Denmark. Danmarks Geologiske Undersøgelse II Række 97, 1–37.

Lee, J.K.W., Williams, I.S. & Ellis, D.J. 1997: Pb, U and Th diffusion in natural zircon. Nature 390, 159–162.

Ludwig, K.R., 2003: Isoplot/Ex 3.00. A geochronological toolkit for Microsoft Excel. Special Publication, vol. 4. Berkeley Geochronological Center, Berkeley, CA.

Mattinson, J.M. 2005: Zircon U–Pb chemical abrasion ("CA-TIMS") method: Combined annealing and multi-step partial dissolution analysis for improved precision and accuracy of zircon ages. Chemical Geology 220, 47– 66.

Micheelsen, H.I. 1961: Bornholms grundfjæld. Meddelelser fra Dansk Geologisk Forening 14, 308–347.

Nasdala, L., Hofmeister, W., Norberg, N., Mattinson, J.M., Corfu, F., Dörr, W., Kamo, S.L., Kennedy, A.K., Kronz, A., Reiners, P.W., Frei, D., Košler, J., Wan, Y., Götze, J,, Häger, T., Kröner, A. & Valley, J.W. 2008: Zircon M257 – a homogeneous natural reference material for the ion microprobe U-Pb analysis of zircon. Geostandards and Geoanalytical Research 32, 247–265.

Obst, K. 2000: Permo-Carboniferous dyke magmatism on the Danish island Bornholm. Neues Jahrbuch für Geologie und Paläontologie Abhandlungen 218, 243–266.

Obst, K., Hammer, J., Katzung, J. & Korich, D. 2004: The Mesoproterozoic basement in the southern Baltic Sea: insights from the G 14-1 off-shore borehole. International Journal of Earth Sciences 93, 1–12.

Pearce, J.A., Harris, N.B.W., Tindle, A.G. 1984: Trace element discrimination diagrams for the tectonic interpretation of granitic rocks. Journal of Petrology 25, 956–983.

Platou, S.W. 1970: The Svaneke Granite Complex and the gneisses on East Bornholm. Bulletin of the Geological Society of Denmark 20, 93–133.

Renne, P.R., Mundil, R., Balco, G., Min, K. & Ludwig, K.R. 2010: Joint determination of ^{40}K decay constants and $^{40}Ar^*/^{40}K$ for the Fish Canyon sanidine standard, and improved accuracy for $^{40}Ar/^{39}Ar$ geochronology. Geochimica et Cosmochimica Acta 74, 5349–5367.

Reno, B.L., Piccoli, P.M., Brown, M. & Trouw, R.A.J. 2012: In situ monazite (U–Th)–Pb ages from the Southern Brasília Belt, Brazil: constraints on the high-temperature retrograde evolution of HP granulites. Journal of Metamorphic Geology 30, 81–112.

Rivera, T.A., Storey, M., Zeeden, C., Hilgen, F. & Kuiper, K. 2011: A refined astronomically calibrated $^{40}Ar/^{39}Ar$ age for Fish Canyon sanidine. Earth and Planetary Science Letters 311, 420–426.

Simon, E., Jackson, S.E., Pearson, N.J., Griffin, W.L. & Belousova, E.A. 2004: The application of laser ablation-inductively coupled plasma-mass spectrometry to in situ U–Pb zircon geochronology. Chemical Geology 211, 47–69.

Sircombe, K.N. 2004: AgeDisplay: an EXCEL workbook to evaluate and display univariate geochronological data using binned frequency histograms and probability density distributions. Computers and Geosciences 30, 21–31.

Sláma, J., Košler, J., Condon, D.J., Crowley, J.L., Gerdes, A., Hanchar, J.M., Horstwood, M.S.A., Morris, G.A., Nasdala, L., Norberg, N., Schaltegger, U., Schoene, B., Tubrett, M.N. & Whitehouse, M.J. 2008: Plešovice zircon – a new natural reference material for U-Pb and Hf isotopic microanalysis. Chemical Geology 249, 1–35.

Stuŵe, K. 2007: Geodynamics of the Lithosphere. Springer: Berlin, Heidelberg, 504 pp.

Tschernoster, R. 2000: Isotopengeochemishe untersuchungen am detritus der Dänisch-Norddeutsch-Polnischen Kaledoniden und deren Vorland. Unpublished Ph.D. thesis, Rheinisch-Westfälischen Technischen Hochschule, Aachen, 128 pp.

Villa, I.M. 1998: Isotopic closure. Terra Nova 10, 42–47.

Waight, T.E., Baker, J.A. & Peate, D.W. 2002a: Sr isotope ratio measurements by double focusing MC-ICPMS: techniques, observations and pitfalls. International Journal of Mass Spectrometry 221, 229–244.

Waight, T.E., Baker, J.A. & Willigers, B.J.A. 2002b: Rb isotope dilution analyses by MC-ICPMS using Zr to correct for mass fractionation: towards improved Rb-Sr geochronology? Chemical Geology 186, 99–116.

Willigers, B.J.A., Krogstad, E.J. & Wijbrans, J.R. 2001: Comparison of thermochronometers in a slowly-cooled granulite terrain: Nagssugtoqidian Orogen, West Greenland. Journal of Petrology 42, 1729–1749.

Willigers, B.J.A., van Gool, J.A.M., Wijbrans, J.R., Krogstad, E.J. & Mezger, K. 2002: Posttectonic cooling of the Nagssugtoqidian Orogen and a comparison of contrasting cooling histories in Precambrian and Phanerozoic Orogens. Journal of Geology 110, 503–517.

Zariņš, K. & Johansson, Å. 2009: U–Pb geochronology of gneisses and granitoids from the Danish island of Bornholm: new evidence for 1.47–1.45 Ga magmatism at the southwestern margin of the East European Craton. International Journal of Earth Science 98, 1561–1580.